UCLouvain

epl

École polytechnique de Louvain

Neuromusculoskeletal Modelling of the Bird

Muscle Stimulation and Reflex-based Control

Author: **Loïc de Schietere de Lophem**
Supervisor: **Renaud Ronsse**
Readers: **Philippe Chatelain, Victor Colognesi, Gennaro Vitucci**
Academic year 2018–2019
Master [120] in Mechanical Engineering

Contents

Abstract

In an effort to understand bird flight and the efficiency optimization mechanisms of migratory birds, the RevealFlight research project studies aerodynamics, mechanics, and control laws of birds. This thesis is part of that project. In particular, it forms the basis of the neural control study. It examines how predetermined movements can be used to generate neural stimulation signals that will allow muscles to recreate those movements. This requires quantifying the forces on the muscles and using the Inverse Hill Model. Finding these stimulation signals allows the use of multiple forms of control to generate movements, rather than having to manually define those movements. Reflex-based Control is one of the possible forms of control and is examined and implemented in this thesis. With Reflex-based Control, sensory information from the muscles is used to generate the stimulation signals. Finally, further improvement points and future research possibilities are identified and suggested.

Chapter 1

Introduction

The RevealFlight Project, of which this Master's Thesis is a part of, is a research project by EPL (Ecole Polytechnique de Louvain) aiming to understand the optimization principles used in bird flight.

"The RevealFlight project aims at shedding light on the efficiency optimization mechanisms deployed by biological flyers. We will focus on birds, and in particular on migratory birds, which are known to exhibit such efficiency-seeking mechanisms at several levels, while maintaining relatively stable flight conditions, leading to impressive results." [1]

Examples of studied mechanisms are flight in formation, aerodynamic properties of the wings, and the biomechanical study of bird flight. This thesis is a part of the latter. It continues on the work of Guillaume Lamine, who studied and wrote his master's thesis (*Musculoskeletal modelling of the bird* [2]) on the kinematics of bird flight and its musculoskeletal model. Using his results, this document examines the neuromuscular phenomena of bird flight. One bird in particular is of interest during this research, the *Geronticus eremita* or Bald Ibis, which is a migratory bird. For now, the flight conditions are limited to a steady-state flight at constant speed and altitude.

The work of Guillaume Lamine is one of the first building blocks of the entire RevealFlight research project. It combines a multibody model with aerodynamic and kinematic ones to make a first flying version of the Bald Ibis. It also studied the main muscles used for bird flight and their integration with the skeleton.

In this thesis, the focus lies in the control of the muscles in order to achieve flight. The stimulations (i.e. the neural signals sent to the muscles) of the different muscles are determined based on the kinematic model already developed. These stimulations are then used to develop Reflex-based Control, where stimulations are generated by using sensory information.

Chapter 2

Method

In order to understand the neuromusculoskeletal aspects of bird flight, as well as the neural control systems used, one can examine the stimulations (neural signals) sent to the muscles. The aim of this project will be to determine the stimulations needed for multiple flight muscles in order to recreate specific movements. In this case, the movements will correspond to wing beats in steady state flight, provided by Guillaume Lamine for his master's thesis [2]. The muscle forces found with the flight kinematics and aerodynamic model will be used in an inverse Hill Muscle Model to determine the stimulations. These will then be compared to reflex-based stimulations. This comparison can give an indication on whether flight control can be reflex based or not.

This chapter will be organized as follows:
First, section 2.1 will give a summary of the available information relevant to this project. This can be information either from the literature, or from the thesis of Guillaume Lamine [2].

Next, section 2.2 explains how to obtain the stimulations that need to be sent to the muscles in order to obtain the muscle forces needed to recreate the movements determined by Guillaume Lamine [2], which allow the bird to fly. More precisely, it will explain how the Inverse Hill Model is used to find the muscle activation (how strongly the muscle is contracting) depending on the force on the Muscle-Tendon Unit (MTU). This is, as the name implies, the muscle and the tendon combined, i.e. what links the different skeletal bones together and pulls on them. The method used for finding this force for each muscle is also explained in this section, as well as how to find the stimulation once the activation is found.

Finally, this section also lists and explains the parameters used in this entire section, as well as where and how they were found.

In section 2.3, the obtained stimulations are used as templates for reflex based control. This is a form of neural control where sensory information is used to determine which stimulation signals need to be sent to the muscles. The principle is explained in more details. The method for determining which sensory information should be used is given there as well.

Finally, it is explained how to go from the sensory information to a stimulation that could be used to make the bird fly.

The last section of this chapter, section 2.4, explains how changes in wingbeat frequency and movement amplitudes are used to validate the robustness of the obtained results.

2.1 Starting Point

As mentioned previously, this project continues on the work done by Guillaume Lamine [2], which provides the Robotran model and Matlab code for flight kinematics, bird dimensions and Muscle-Tendon Unit (MTU) forces.

Concerning the stimulation signals sent to the muscles, multiple generation principles exist.

Central Pattern Generators (CPG) produce a rhythmic output without a rhythmic input [7]. This could, for example, have an input for the desired flight speed, while the outputs are the corresponding cyclic signals sent to the muscles in order to achieve this speed. This has been used for human walking gait by Van der Noot [3].

Reflex-based Control uses different sensory information (e.g. muscle force, muscle length, ...) to find the muscle stimulation and achieve specific movements [5], in this case flight. This makes it possible to take perturbations into account, which is not possible with the simple inputs of the CPG. An optimal model would combine a CPG, for steady state flight, with Reflex-based Control, for perturbations. Additionally, CPGs are typically used for proximal muscles (close to the torso), not for distal muscles (far from the body) [3].

This project will focus on Reflex-based Control rather than CPGs for multiple reasons.

First of all, CPGs are much more complex than Reflex-based Control, as they

require a network of oscillators and more demanding optimization.

Additionally, since there is no reference stimulation to match yet, one would have to use the non-optimized, temporary stimulations to find the muscle forces with the Hill Muscle Model, run the code to ensure flight stability, and finally find the optimal stimulations out of all the stable ones. This is too much for a first approach of the problem.

Finally, the goal of the work by Van der Noot [3] is to find an optimal gait without guidance, while the goal of this project is to match an existing set of movements.

The choice has thus been made to start by finding the stimulations needed to match the given flight kinematics by using the Inverse Hill Method. The possibility for Reflex-based Control is then evaluated.

2.1.1 Model and Kinematics

This project started with a Robotran model and a Matlab code made by Guillaume Lamine [2]. The Robotran model contains a representation of the bird skeleton, with the correct bone lengths. The bone movements are defined in Matlab. The wing interaction with the air is computed with a basic aerodynamic model. This model is used to verify that the flight is stable (constant altitude and forward speed) and to find the torque at the joints.

A bird wing contains many muscles to obtain smooth and precise wing control. In order to simplify the problem, the number of muscles used in this model has been limited to 10:

- *Pectoralis* (PT): Main flight muscles for the bird. Lowers the wing and adducts the shoulder (brings the wing backwards). Links the bird body and the upper arm. This is the main source of power for lift and thrust.
- *Supracoracoideus* (SC): Antagonist of PT. Raises the wing and abducts the shoulder (brings the wing forwards). Links the body and the upper arm.
- *Scapulohumeralis Caudalis* (SHC): Adducts the shoulder and raises the wing. Links the body and the upper arm.
- *Coracobrachialis Caudalis* (CBC): Abducts the shoulder and lowers the wing. Links the body and the upper arm.
- *Extensor Metacarpi Radialis* (EMR): Radial deviation of the wrist (rotate forwards). Links the upper arm and the hand.

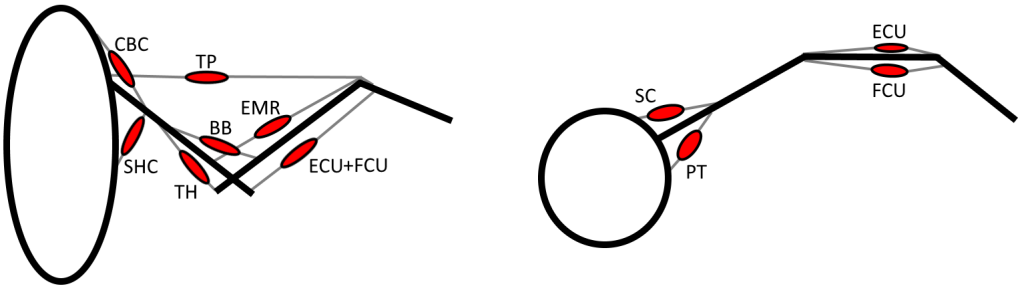

(a) Top view (b) Frontal view

Figure 2.1: Simplified muscle layout of the wing.

- *Flexor Carpi Ulnaris* (FCU): flexes the wrist (rotates the wrist downwards) and causes ulnar deviation (rotate backwards). Links the upper arm and the hand.
- *Tensor Propatagialis* (TP): Radial deviation of the wrist (rotate forwards). Links the body and the hand.
- *Extensor Carpi Ulnaris* (ECU): Extends the wrist (rotates the wrist upwards) and causes ulnar deviation (rotate backwards). Links the upper arm and the hand.
- *Biceps Brachii* (BB): Flexes the elbow. Links the upper and lower arm.
- *Triceps Brachii Humeral Head* (TH): Extends the elbow. Links the upper and lower arm.

A simplified schematic of the muscle layout is given in figure 2.1.

Each wing has 7 possible joint rotations in the Robotran model: 3 for the shoulder, 2 for the elbow (flexing/extending and twisting), and 2 for the wrist (flexing/extending and radial/ulnar deviation). This is shown in figure 2.2.

However, multiple degrees of freedom are locked in the Matlab model, in order to simplify the kinematics. The only non-constant joint rotations are the two wrist movements and the main beating movement at the shoulder (which lowers and raises the wing).

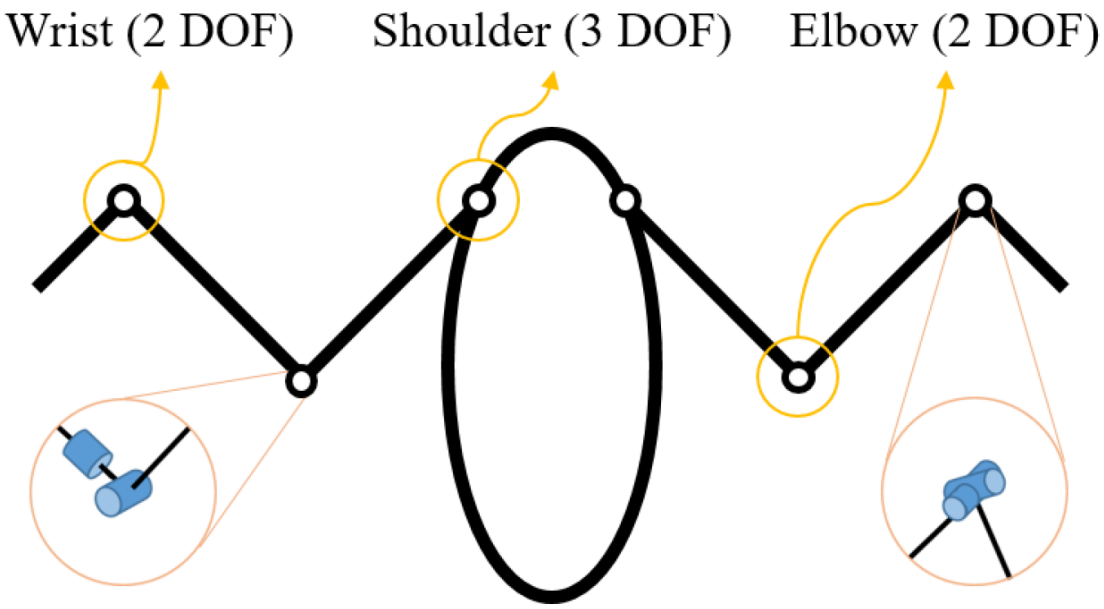

Figure 2.2: Wing degrees of freedom. Picture from Lamine [2]

2.2 Muscle Stimulations

This section will explain how the reference stimulations are obtained. These stimulations are the signals sent to the muscle. They can be found once the muscle activations are known, as explained in section 2.2.4.

The muscle activation represents, on a scale from 0 to 1, how strongly the muscle is activated compared to its maximum capacity. This is found with the Inverse Hill Model, as explained in section 2.2.1.

This model needs data before it can be used. The origin of most of the data, coming from the literature, is given in section 2.2.2.

Other values are taken from the kinematics analysis. The way this is done for the muscle forces is explained in section 2.2.3

2.2.1 Inverse Hill Model

The Hill Model is a way to model muscles, in particular Muscle Tendon Units (MTU). These are units containing a muscle and the corresponding tendons attaching it to the bones. The representation of these MTUs is shown on figure 2.3. In regular operation, an active, Contractile Element (CE) is in series with an elastic Series

Element (SE). It is the CE that provides power to the muscle by contraction. The elastic Parallel Element (PE) engages when the CE elongates to more than its optimum length ($l_{ce} > l_{opt}$). On the other hand, the elastic Buffer Element (BE) prevents the CE from collapsing when the SE is slack ($l_{MTU} - l_{ce} < l_{slack}$) [6]. In this flight scenario, the PE and BE elements are not necessary, since it is safe to assume that in steady-state flight the muscles will stay in their designed length range. However, PE and BE are still included in this model, both for completeness and to be able to verify that their forces stay zero at all times.

This figure 2.3 shows that the force on the MTU, F_m, is

$$F_m = F_{se} = F_{ce} + F_{pe} - F_{be}$$

A detailed explanation of how to use this model to find F_m starting from the muscle stimulation is given in (Geyer et al. 2010 [6]). Since, in this thesis, the stimulation is the objective and the MTU force is given (see section 2.2.3), the Inverse Hill Model is used.

When the force of the Series Element (SE) is known ($F_{se} = F_m$), it can be used to find the length of the SE:

$$l_{se} = \epsilon_{ref} l_{slack} \sqrt{\frac{F_{se}}{F_{max}}} + l_{slack}$$

where F_{max} is the maximum force output of the muscle and ϵ_{ref} is a reference strain.

The values for the different parameters will be given in section 2.2.2.

The length of the Contractile Element (CE) can now be found, since

$$l_{ce} = l_{MTU} - l_{se}$$

where l_{MTU} is known from the kinematics analysis. With l_{ce} known for every timestep, the CE velocity can be found:

$$v_{ce} = \frac{dl_{ce}}{dt}$$

It is now possible to find F_{pe} and F_{be}, needed to obtain F_{ce}:

$$F_{pe} = F_{max} f_{pe}(l_{ce}) f_v(v_{ce})$$

where $f_v(v_{ce})$ is the force-velocity relationship and

$$f_{pe}(l_{ce}) = \begin{cases} \left(\frac{l_{ce} - l_{opt}}{l_{opt}\epsilon_{pe}}\right)^2 & \text{if } l_{ce} > l_{opt} \\ 0 & \text{if } l_{ce} \leqslant l_{opt} \end{cases}$$

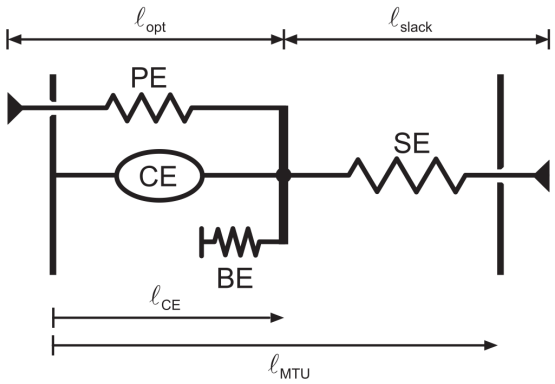

Figure 2.3: Hill Muscle Model representation. In regular operation, an active, Contractile Element (CE) is in series with an elastic Series Element (SE). The elastic Parallel Element (PE) engages when the CE elongates to more than its optimum length ($l_{ce} > l_{opt}$). On the other hand, the elastic Buffer Element (BE) prevents the CE from collapsing when the SE is slack ($l_{MTU} - l_{ce} < l_{slack}$) [6].

$$f_v(v_{ce}) = \begin{cases} \frac{v_{max} - v_{ce}}{v_{max} + K v_{ce}} & \text{if } v_{ce} < 0 \\ \frac{N + (N-1)(v_{max} + v_{ce})}{7.56 K v_{ce} - v_{max}} & \text{if } v_{ce} \geqslant 0 \end{cases}$$

$$F_{be} = \begin{cases} \left(\frac{l_{min} - l_{ce}}{l_{opt} \epsilon_{be}} \right)^2 & \text{if } l_{ce} < l_{min} \\ 0 & \text{if } l_{ce} \geqslant l_{min} \end{cases}$$

$$F_{ce} = F_m + F_{be} - F_{pe}$$

The final step before finding the muscle activation is to find f_l, the force-length relationship:

$$f_l(l_{ce}) = \exp \left[c \left| \frac{l_{ce} - l_{opt}}{w} \right|^3 \right]$$

The activation $A_m(t)$ is given by:

$$A_m(t) = \frac{F_{ce}}{F_{max} f_l(l_{ce}) f_v(v_{ce})}$$

2.2.2 Starting Data

Little muscular and neural data are available for our bird of interest, the Bald Ibis. This is important to keep in mind. However, since the aim of this thesis is to develop a methodology, the exact values of parameters are not as important, as

long as a critical view of the results is kept. Parameter values can be changed later when available, if more precise results are required.

This section will explain where the starting data comes from and how it was adapted to fit the Bald Ibis.

The values of l_{MTU} and F_m are found from the kinematics analysis performed in Matlab with the Robotran model. More information about the extraction of F_m will be given in section 2.2.3.

Some information that is not available for Bald Ibises, did exist for other birds, for example the Golden Pheasant [8]. These include the maximal muscle force F_{max}, the optimal CE length l_{opt} (which corresponds to the resting belly length [9]), and the tendon length l_{slack} for each muscle. In order to use them for the Bald Ibis rather than the Golden Pheasant, conversion constants are used. For F_{max} the mass ratio of the birds is used, since a heavier bird needs stronger muscles to lift its mass. The ratio obtained is 2.84 [8, 10]. This ratio is used to multiply the values given for the Golden Pheasant in order to obtain approximations for the Bald Ibis.

For l_{opt} and l_{slack} the ratio between muscle and tendon is conserved from pheasant to ibis. The sum of the lengths is set to be equal to the maximum value of the MTU length according to the Matlab model. This ensures that the muscles stay in regular operation range (i.e. muscle is not too long or too short, $l_{ce} > l_{opt}$ and $l_{MTU} - l_{ce} < l_{slack}$, see section 2.2.1), which is expected in steady state flight.

The obtained values for the maximum muscle force F_{max}, optimal muscle length l_{opt}, and slack tendon length l_{slack} are given in table 2.1.

Other required data, mainly muscular and neural properties, were not available for any bird. They have thus been taken and adapted if needed from studies of the human gait (walking) [5, 6]. The parameters are listed in table 2.2. These values need to be taken with a grain of salt, since there are differences between the phenomena present in human walking and in bird flight. For example, the excitation-contraction coupling (phenomenon between the stimulation signal being sent and the muscle contracting) happens differently for mammals and non-mammalian vertebrates [13]. This may lead to a different value of τ. However, since the values are reasonable and no better values have been found, these are used.

The meanings of the different parameters given in table 2.2 are given here [5, 6].

- The force-length relationship $f_l(l_{ce})$ described for the Inverse Hill Model

Muscle	$F_{max}[N]$	$l_{opt}[m]$	$l_{slack}[m]$
Pectoralis (PT)	952.6	0.1267	0.0135
Supracoracoideus (SC)	309.9	0.114	0.014
Scapulohumeralis Caudalis (SHC)	136.5	0.085	0.012
Coracobrachialis Caudalis (CBC)	91	0.069	0.012
Extensor Metacarpi Radialis (EMR)	54	0.097	0.098
Flexor Carpi Ulnaris (FCU)	68.2	0.116	0.019
Tensor Propatagialis (TP)	17.1	0.205	0.079
Extensor Carpu Ulnaris (ECU)	22.7	0.095	0.061
Biceps Brachii (BB)	71.1	0.090	0.036
Triceps Brachii Humeral Head (TH)	88.2	0.077	0.028

Table 2.1: Maximum force, optimal muscle length and slack tendon length for each muscle of the Bald Ibis used in the simulations.

(section 2.2.1) is a bell-shaped curve. w is the width of the curve.

- c is then defined as $c = log(0.05)$ so that $f_l(l_{opt}(1 \pm w)) = 0.05$ is fulfilled.
- l_{min} is, as explained previously, the minimum length the Contractile Element (CE) of the muscle model can have before the Buffer Element (BE) starts to generate a force. This force is needed to stop the muscle from buckling. In normal muscle use, the BE should not be necessary, but it is still implemented in this model for completeness.
- The parameter v_{max} represents the maximum shortening velocity of the muscle.
- ϵ_{ref}, ϵ_{pe}, and ϵ_{be} are the strains of the SE, the PE, and the BE respectively.
- τ is the extraction-contraction correlation constant, and links the delay between the stimulation and the muscle activation.
- K is the curvature constant for the hyperbolic function for the force-velocity relationship f_v.
- The eccentric force enhancement N is the relative amount of force on the MTU compared to the maximum muscle force $\left(\frac{F_{MTU}}{F_{max}}\right)$ when the maximum lengthening velocity is reached ($v_{ce} = -v_{max}$).

Parameter	Value
w	$0.56\, l_{opt}\ [m]$
l_{min}	$(l_{opt} - w)\ [m]$
v_{max}	$-12\, l_{opt}\ \left[\frac{m}{s}\right]$
ϵ_{ref}	$0.04\ [-]$
ϵ_{pe}	$\frac{w}{l_{opt}}\ [-]$
ϵ_{be}	$\frac{1}{2}\frac{w}{l_{opt}}\ [-]$
τ	$0.01\ [s]$
K	$5\ [-]$
N	$1.5\ [-]$
c	$log(0.05)\ [-]$

Table 2.2: Data for the Hill Model taken from (Geyer et al. 2010 [6]).

2.2.3 Muscle-Tendon Unit Force

In order to find the desired muscle stimulations, it is necessary to invert the Hill Muscle Model. This will give the muscle activation when the Muscle Tendon Unit (MTU) force is known (see section 2.2.1). This force is found by using the joint torque and the lever arm of each muscle. Both can be found with the kinematics simulations.

$$\underline{\tau} = \underline{\underline{R}} \cdot \underline{F} \tag{2.1}$$

where $\underline{\tau} \in \mathbb{R}^{7\times1}$ and $\underline{\underline{R}} \in \mathbb{R}^{7\times10}$ are given by Lamine [2] and $\underline{F} \in \mathbb{R}^{10\times1}$ is F_{MTU} for each muscle. This is what is needed for this thesis, in order to use the Inverse Hill Model.

This results in an underdetermined system of 7 equations and 10 unknowns. Extra conditions are thus needed to solve it. The solution used is to minimize the sum of relative forces of the muscles with quadratic programming:

$$\sum_{i=1}^{10} \left(\frac{F_{m,i}}{F_{max,i}} \right)^2$$

while satisfying equation 2.1.

Linear programming could not be used, due to the antagonist muscles used. If a force is needed in one direction, only muscles active in the same direction will be used, while the antagonists have a zero force. This reduces the number of unknowns, giving a determined system. Because of this, no optimization can happen, resulting in forces being potentially higher than their maximum possible value F_{max}. With quadratic programming, the antagonists will have small but

non-zero values, making optimization possible.

Upper and lower bounds can be given to the forces. A first solution is to put the lower bound at zero, since muscle forces can not be negative, and the upper bound at F_{max}. However, this can give muscle activations outside of the accepted range ($0 \leqslant A_m(t) \leqslant 1$). This is because the forces computed here are for the MTU, not the muscle itself.

When the force generated by the CE of the Hill Model is zero, passive elements, which can be considered as springs (e.g. Parallel Element PE), can still generate a force if the muscle is outside of the standard range. If the optimization gives a zero force for the MTU, it would result in a negative force by the CE, which is not biological.

While this scenario is not possible by definition of the muscle and tendon length in this model, it can still be necessary to keep this potential problem in mind if the parameter values are chosen differently. To solve this issue, one can change the lower bound of the quadratic programming to be the highest value between 0 and F_{pe}. This way, when the minimum value for the MTU force is obtained, the CE force will be zero rather than negative.

Similarly, the upper bound may need to be modified. This will be necessary for muscles that reach their maximum force. Since the activation is given by $A_m(t) = \frac{F_{ce}}{F_{max} f_l(l_{ce}) f_v(v_{ce})}$, the activation is higher than 1 when $F_{ce} = F_{max}$ if $f_l(l_{ce}) f_v(v_{ce})$ is lower than 1. In this model, it has been observed that $f_l(l_{ce})$ stays close to 1 for the muscles reaching their maximum force value. This may not be the case for different parameter values. The solution to the problem was then to change the upper bound to the minimum value between F_{max} and $F_{max} f_v(v_{ce})$.

2.2.4 Stimulation

The stimulations can be found with the muscle activations. The stimulations are the signals sent by the nervous system to the muscles. The intensity of the signals goes from 0 to 1. The activations are a representation of how strongly the muscle is contracting. This is also shown on a continuous scale from 0 (no activation) to 1 (maximum activation). Due to reflex time and other delays, the muscle is not activated immediately after the signal is sent. Additionally, high frequency changes in the stimulation will have a reduced impact on the activation. The muscle activation can thus be seen as a the output of a low-pass filter with the

stimulation as input. This is represented in the following differential equation [5]:

$$\tau \frac{dA_m(t)}{dt} = S(t) - A_m(t)$$

where $S(t)$ is the stimulation and τ is a time constant. With $A_m(t)$ and τ known (from sections 2.2.1 and 2.2.2 respectively), the stimulation can easily be found.

$$S(t) = \tau \frac{dA_m(t)}{dt} + A_m(t)$$

2.3 Reflex-based Control

2.3.1 Principle

The stimulation is made up of a constant stimulation bias S_0 and feedback from sensory information $\pm GP(t - \Delta_P)$ [5]:

$$S(t) = S_0 \pm GP(t - \Delta_P) \tag{2.2}$$

where G is a constant, positive gain, P is the sensory information, and Δ_P is the signal-propagation time delay.

The feedback from sensory information is negative when it inhibits stimulation, and positive when it excites it. Multiple types of sensory information can be chosen for P. In this thesis, six are chosen to be studied: The MTU force, the CE length, and the CE velocity, on both the studied muscle and the antagonist. A list of the muscles and their antagonists is listed in table 2.3. The antagonist of some muscles is not as obvious as for others. The muscles chosen work in multiple directions on multiple degrees of freedom, but not always in pairs. The antagonists given in table 2.3 when doubt is possible are the ones that are active at complementary times as much as possible.

Combinations of P signals are not studied. A condition existing for P is that is must be positive. This is due to the mechanism at play for neural information transfer [5]. For the length and velocity signals a constant offset value is subtracted: $P = l_{CE} - l_{off}$ and $P = v_{CE} - v_{off}$. The reason for this is that the information is given by the muscle spindle, i.e. stretch receptors that detect changes in muscle length rather than absolute length [14, 5]. This is not the case for the force signal.

Muscle	Antagonist
Pectoralis (PT)	SC
Supracoracoideus (SC)	PT
Scapulohumeralis Caudalis (SHC)	CBC
Coracobrachialis Caudalis (CBC)	SHC
Extensor Metacarpi Radialis (EMR)	ECU
Flexor Carpi Ulnaris (FCU)	TP
Tensor Propatagialis (TP)	FCU
Extensor Carpu Ulnaris (ECU)	EMR
Biceps Brachii (BB)	TH
Triceps Brachii Humeral Head (TH)	BB

Table 2.3: Muscles and their antagonists

2.3.2 Correlation and Delay

Since it is not known in advance which sensory information P will give good results, all sensory information needs to be compared. The relation between $P(t - \Delta_P)$ and the stimulation is linear (see equation 2.2). We can thus study the correlation between both. The constant offsets and the gain do not influence this correlation, since they are parameters of the linear relationship. The delay does have an influence. The exact value of this is not known either, but a typical value is about 30 ms [5]. The correlations are then tested with delays of 5 to 50 ms. This delay means that P, the sensory information, is in advance on the stimulation.

The correlations for each sensory information are then compared per muscle. The ones with the best correlation for any delay are then taken for further analysis. Obviously in these cases the optimal delay is where the correlation had the maximum value. Muscles where no correlation coefficient reaches an arbitrary limit value of 0.5 in absolute value (0 is no correlation, -1 and 1 are perfect correlations, where negative values mean an opposite relationship) within the delay range are omitted.

2.3.3 Stimulation Bias and Gain

Once the muscles and sensory information are selected along with their respective delays, the three remaining unknowns can be found: the gain G, the stimulation bias S_0, and, in the case of the length and velocity information, the offset value P_{off}. In a first phase, the two latter values will be considered as a single constant, C. They will later be separated.

The goal is to determine the values of C and G that give the best match with the original stimulation found in section 2.2.4. The best match is defined as minimizing

$$\sum_{t=t_{start}}^{t_{end}} |S(t) - S'(t)|$$

where $S'(t)$ is the new stimulation, and t_{start} and t_{end} are the start and end times of a chosen time interval. This interval should at least contain one full cycle. The different $S'(t)$ are generated with $S'(t) = C \pm GP(t - \Delta_P)$, where C and G take on a wide range of values. When the best match with the original stimulation is found, the corresponding values for C and G are recorded. It is important to note that, while $S(t)$ can not be lower than 0, This method could give results that do not satisfy this condition. In some cases, it was necessary to exclude the stimulations that had a better match with the original one, but had a significant negative part. The limit for this consideration is set at -0.001, since minor negative values will not have a large impact, the excess will be ignored.

It is now necessary to split the constant C into the stimulation bias S_0 and the offset values P_{off} for the length and velocity information. They are linked to C by:

$$C = S_0 \mp GP_{off}$$

where C and G are known. This can be rewritten as

$$P_{off} = -\frac{C - S_0}{G} \tag{2.3}$$

where G can be either positive or negative depending on the sign in equation 2.2. We would need a second equation in order to find both unknowns. There is no information about what these values should be or how they are related. However, S_0 can not be exactly zero due to the function it fulfills, and in (Geyer et al. 2003 [5]) and (Geyer et al. 2010 [6]) it has values of 0.01 and up. It has thus been chosen that S_0 can not have a value lower than 0.01. In table 3.2 the cases where forces are used as sensory information have $C = 0.01$. The forces do not have an offset value P_{off}, meaning that $C = S_0$. If the constraint $S_0 \geqslant 0.01$ is not implemented, the stimulation bias becomes exactly zero, which is not possible.

From this observation, it has been chosen to set $S_0 = 0.01$ as the default value in all cases where the gain is positive. When the gain is negative (corresponding to inhibitory signals), the stimulation bias is set to $S_0 = 0.99$. With these values it is possible to find P_{off} with equation 2.3. However, this may, in some cases, result in P_{off} being greater than the minimum value of $l_{ce}(t)$, which means that the condition $P(t) = l_{ce}(t) - l_{off} \geqslant 0$ is not satisfied. In those cases, the value of S_0 is increased (or decreased) until l_{off} equals the minimum value of $l_{ce}(t)$, thus satisfying the constraint. The new stimulation, based on reflexes, is now fully defined.

2.4 Flight Parameter Sensitivity

In this section, the robustness of this model towards changes in flight parameters (more exactly flight speed) is examined. Wingbeat frequencies are changed, which leads to changes in amplitude in order to maintain stable flight. In practice, the frequency of all movements is increased or decreased by 20%. The amplitudes of these movements are then changed by the percentage needed to achieve stable flight (found by trial and error until the altitude and horizontal speed were constant). However, this change in amplitude (around 6%) is relatively low. For this reason, two extra sets of data are added, where the amplitude is changed by 20%.

It is possible, since the movements remain similar between all cases, to predict likeness for the graphs of forces and lengths. The exact values will be different, but the general trends will be conserved. The parameters of the reflex-based stimulations will be different for each case as well. The delay, however, is a physiological property of the bird, and should remain constant between all scenarios. This needs to be verified.

Chapter 3

Results

In this chapter, the results of the different simulations will be given. They will be discussed in chapter 4.

3.1 Muscle Force, Activation and Stimulation

Figure 3.1 shows the muscle force, activation and stimulation of the muscles. For some muscles, the stimulation goes outside its allowed range of $0 \leqslant S(t) \leqslant 1$ for short periods of time. This is because, in the Inverse Hill Model, the stimulation is found by deriving the activation. This leads to high stimulation values where the activation is non-differentiable. For the rest of the analysis, the stimulations are artificially limited to $0 \leqslant S(t) \leqslant 1$. This will give cleaner results, while not changing the observations to be made. Since the spikes are so narrow, the impact of removing them will be negligible.

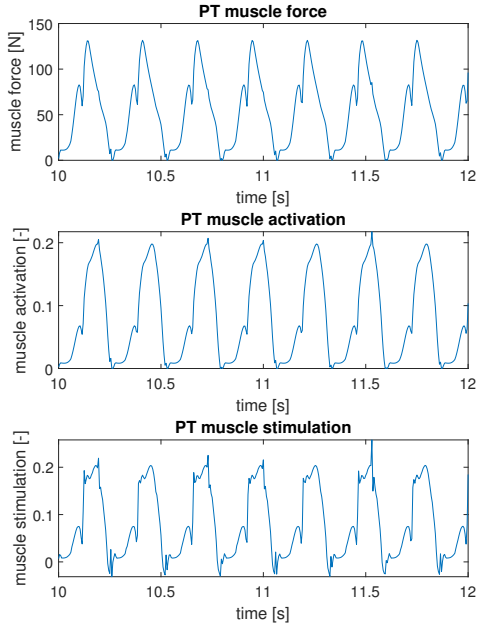
PT muscle force
muscle force [N]
150
100
50
0
10
10.5
11
11.5
12
time [s]
PT muscle activation
muscle activation [-]
0.2
0.1
0
10
10.5
11
11.5
12
time [s]
PT muscle stimulation
muscle stimulation [-]
0.2
0.1
0
10
10.5
11
11.5
12
time [s]

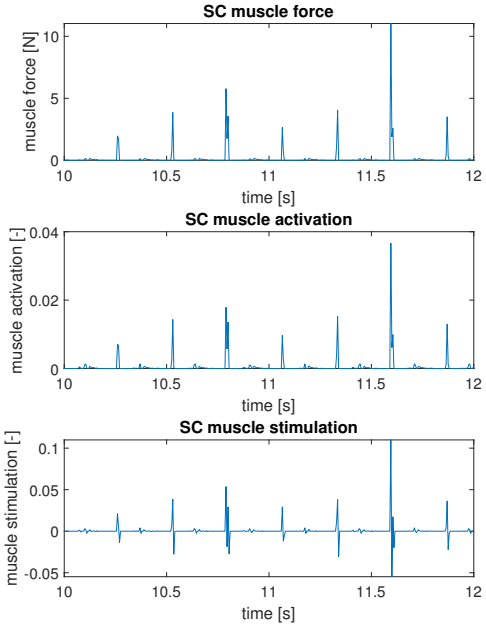
SC muscle force
muscle force [N]
10
5
0
10
10.5
11
11.5
12
time [s]
SC muscle activation
muscle activation [-]
0.04
0.02
0
10
10.5
11
11.5
12
time [s]
SC muscle stimulation
muscle stimulation [-]
0.1
0.05
0
-0.05
10
10.5
11
11.5
12
time [s]

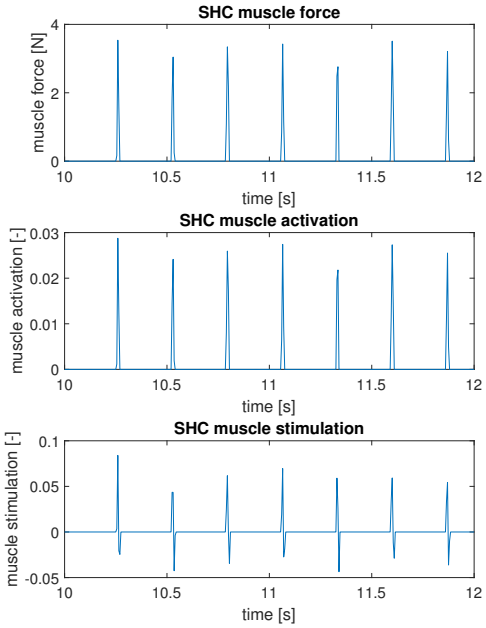
SHC muscle force
muscle force [N]
4
2
0
10
10.5
11
11.5
12
time [s]
SHC muscle activation
muscle activation [-]
0.03
0.02
0.01
0
10
10.5
11
11.5
12
time [s]
SHC muscle stimulation
muscle stimulation [-]
0.1
0.05
0
-0.05
10
10.5
11
11.5
12
time [s]

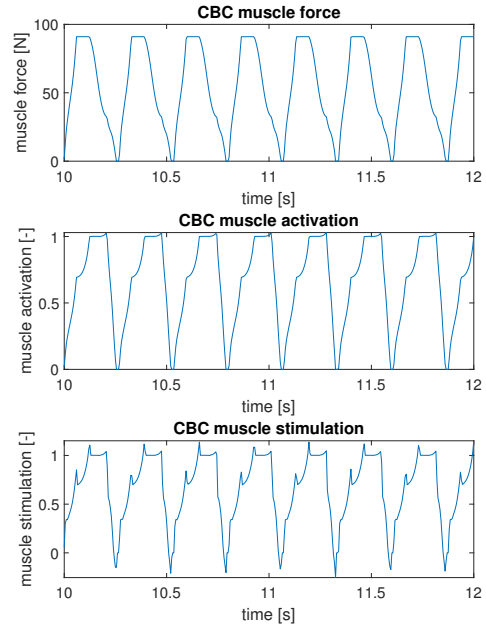
CBC muscle force
muscle force [N]
100
50
0
10
10.5
11
11.5
12
time [s]
CBC muscle activation
muscle activation [-]
1
0.5
0
10
10.5
11
11.5
12
time [s]
CBC muscle stimulation
muscle stimulation [-]
1
0.5
0
10
10.5
11
11.5
12
time [s]

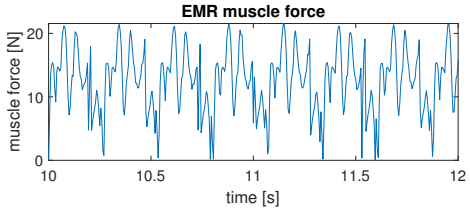
EMR muscle force
muscle force [N]
time [s]

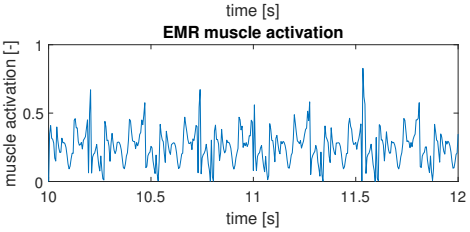
EMR muscle activation
muscle activation [-]
time [s]

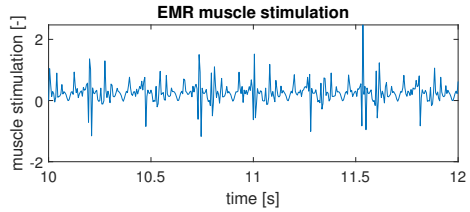
EMR muscle stimulation
muscle stimulation [-]
time [s]

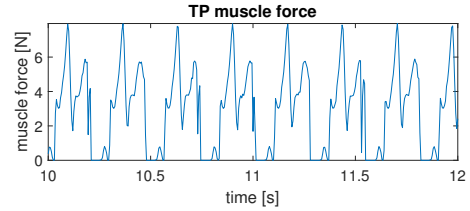
TP muscle force
muscle force [N]
time [s]

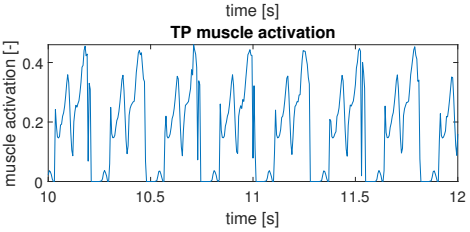
TP muscle activation
muscle activation [-]
time [s]

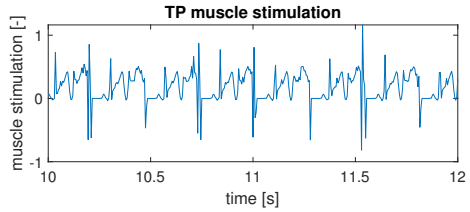
TP muscle stimulation
muscle stimulation [-]
time [s]

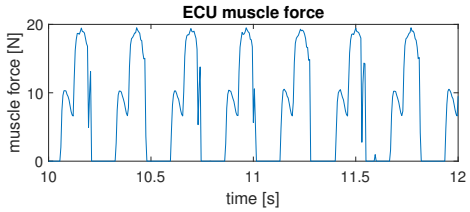
ECU muscle force
muscle force [N]
time [s]

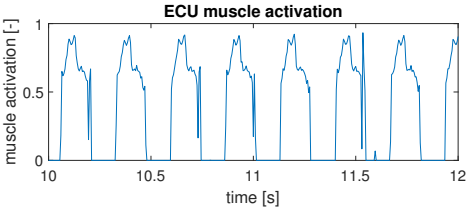
ECU muscle activation
muscle activation [-]
time [s]

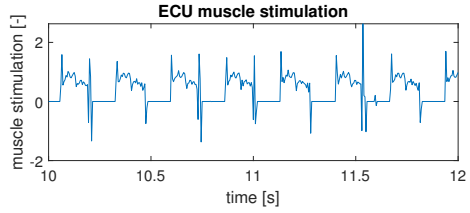
ECU muscle stimulation
muscle stimulation [-]
time [s]

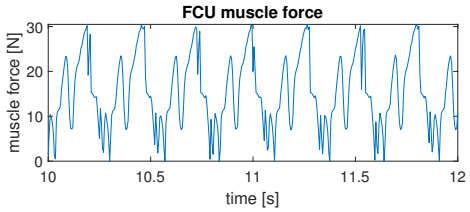
FCU muscle force
muscle force [N]
time [s]

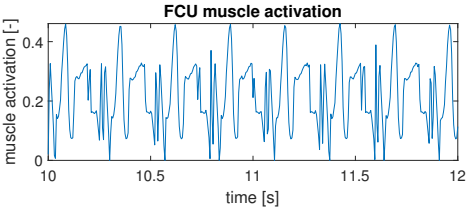
FCU muscle activation
muscle activation [-]
time [s]

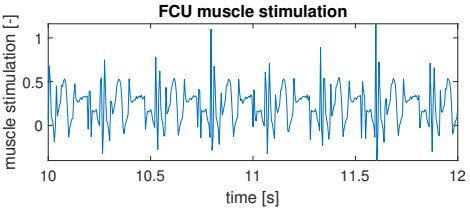
FCU muscle stimulation
muscle stimulation [-]
time [s]

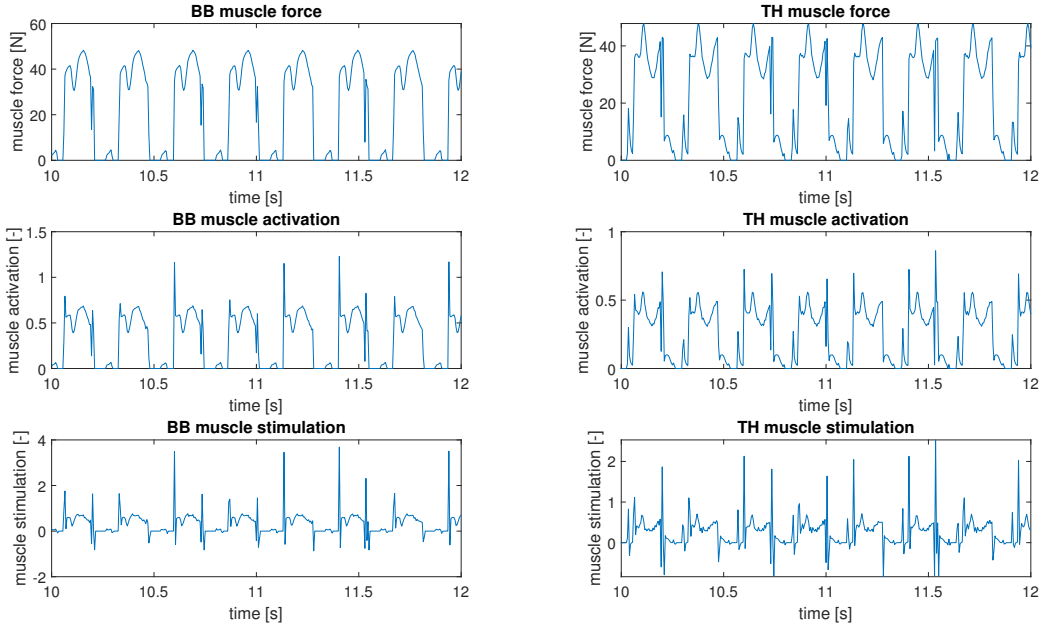

Figure 3.1: Muscle force, activation and stimulation results of all studied muscles. The time ranges from 10 to 12 seconds after the start of the simulation, in order to ensure steady-state conditions.

3.2 Reflex-based Control

3.2.1 Correlation and Delay

The correlations for a range of delays and sensory information is given for each muscle in figure 3.2. The considered delays range between 5 and 50 ms, but the graphs show the results for delays between 0 and 60 ms. This is to have a better idea of trends outside of this range. The correlations themselves go from -1 to 1. The goal of the analysis is double: to find which sensory information give the closest result to the original stimulation, and to find what the optimal delay is for that feedback loop. As a reminder, the best sensory information and delay have the absolute value of the correlation closest to 1. The results are summarized in table 3.1.

Muscle	Sensory Information	Delay [ms]	Correlation [-]
PT	Antagonist CE Length	45	-0.94
SC	/	/	/
SHC	/	/	/
CBC	CE Length	10	0.92
EMR	/	/	/
FCU	/	/	/
TP	CE Length	35	0.57
ECU	Antagonist CE Length	50	-0.79
BB	MTU Force	5	0.70
TH	Antagonist MTU Force	10	0.57

Table 3.1: Summary of the best sensory information and delay for each muscle, as well as the corresponding correlation value. When the value of all sensory information are below 0.5 in absolute value, the muscles are not considered for further analysis.

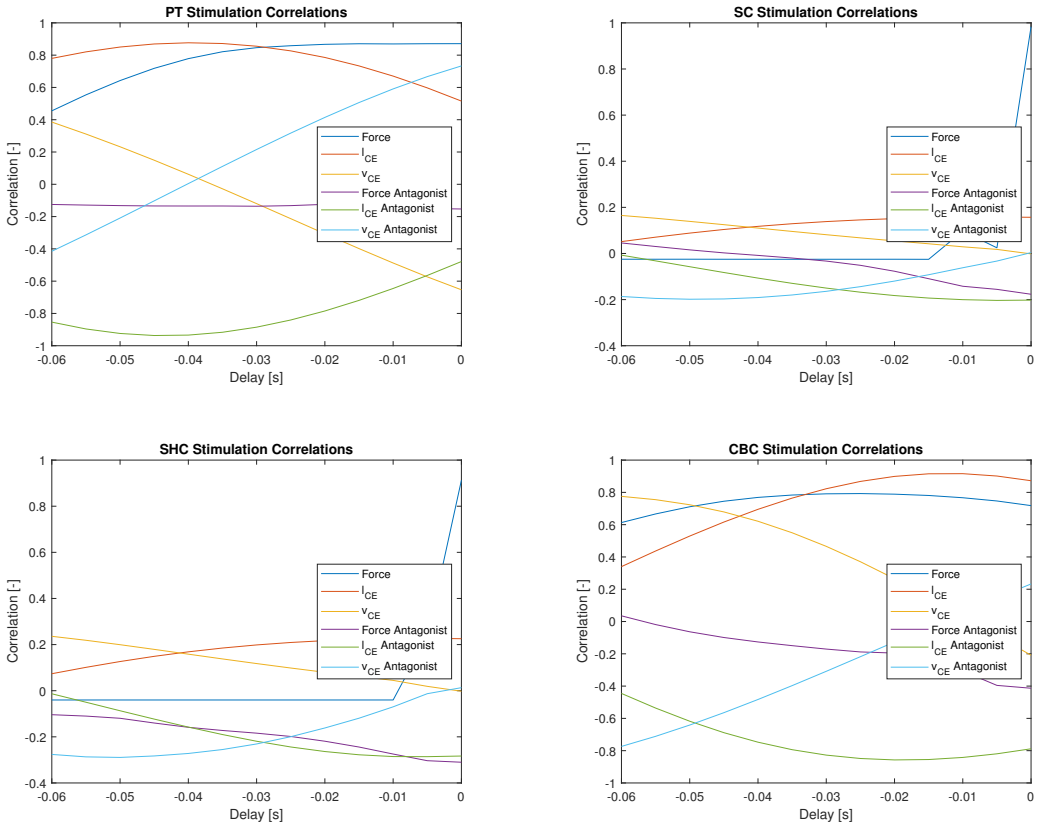

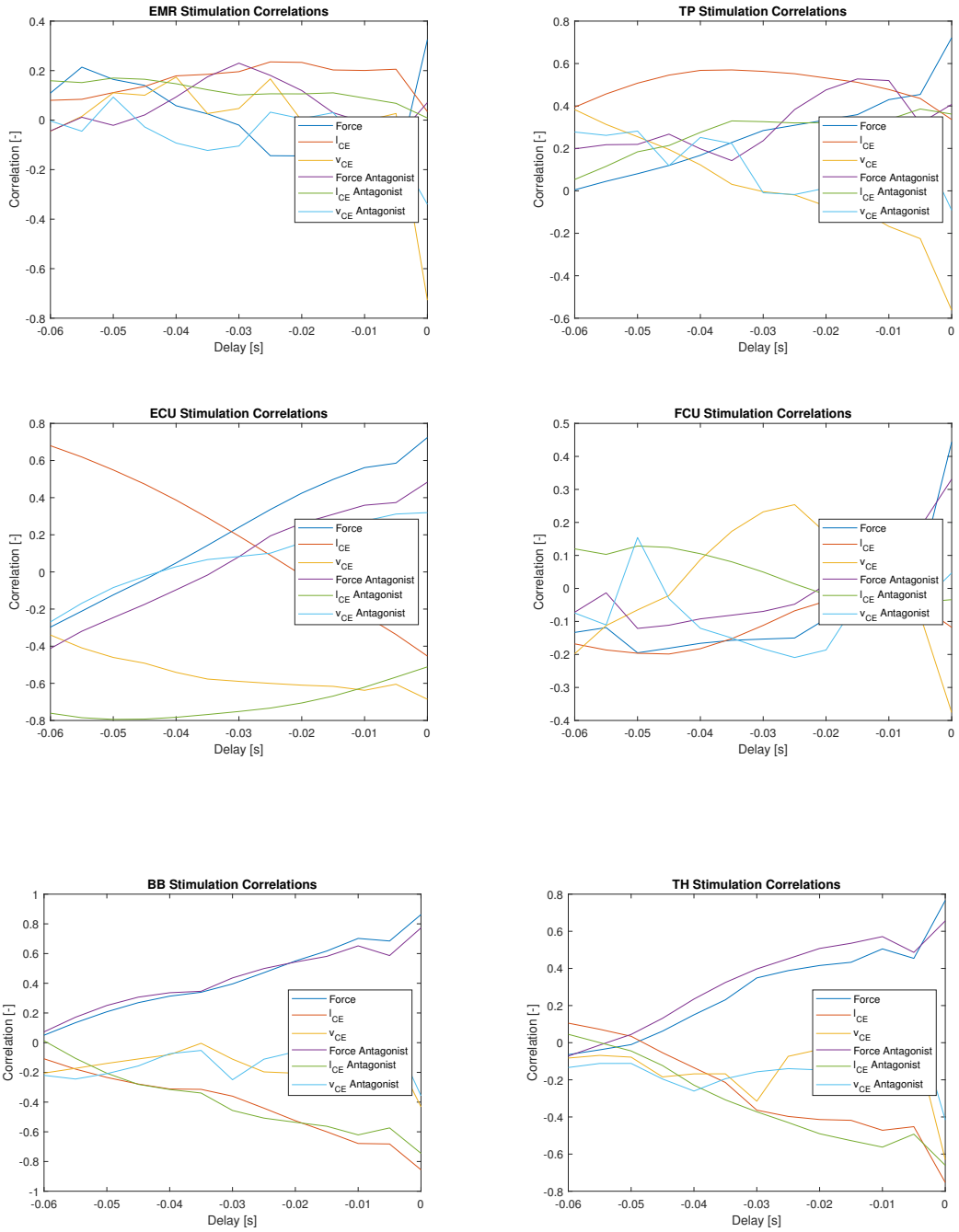

Figure 3.2: For each muscle, the correlation (y-axis) is given for a range of delays (x-axis) between the stimulation and the different studied sensory information: The force, length, and velocity of the muscle and its antagonist.

3.2.2 Stimulation Bias and Gain

For the muscles selected with the results of section 3.1 and their respective sensory information, the computation of the different constants can be found, as explained in section 2.3.3. As a reminder, C and G are found first. Afterwards, C is split into S_0 and P_{off}. All the values obtained for these parameters are shown in table 3.2.

Muscle	G	C[-]	S_0 [-]	P_{off}
PT	$-5.72[m^{-1}]$	0.66	0.196	$0.081[m]$
CBC	$57.41[m^{-1}]$	-2.92	0.25	$0.055[m]$
TP	$52.43[m^{-1}]$	-10.26	0.01	$0.196[m]$
ECU	$-78.56[m^{-1}]$	9.12	0.99	$0.104[m]$
BB	$0.0135[N^{-1}]$	0.01	0.01	$0[N]$
TH	$0.0094[N^{-1}]$	0.01	0.01	$0[N]$

Table 3.2: Numerical values of the stimulation parameters. Note that only six muscles are shown, since the other four did not have a high enough correlation as shown in table 3.1.

3.2.3 Resulting Stimulations

The stimulations found for the Reflex-based Control, for the selected muscles and their corresponding sensory information is compared to the stimulation found by the Inverse Hill Model. This is shown in figure 3.3.

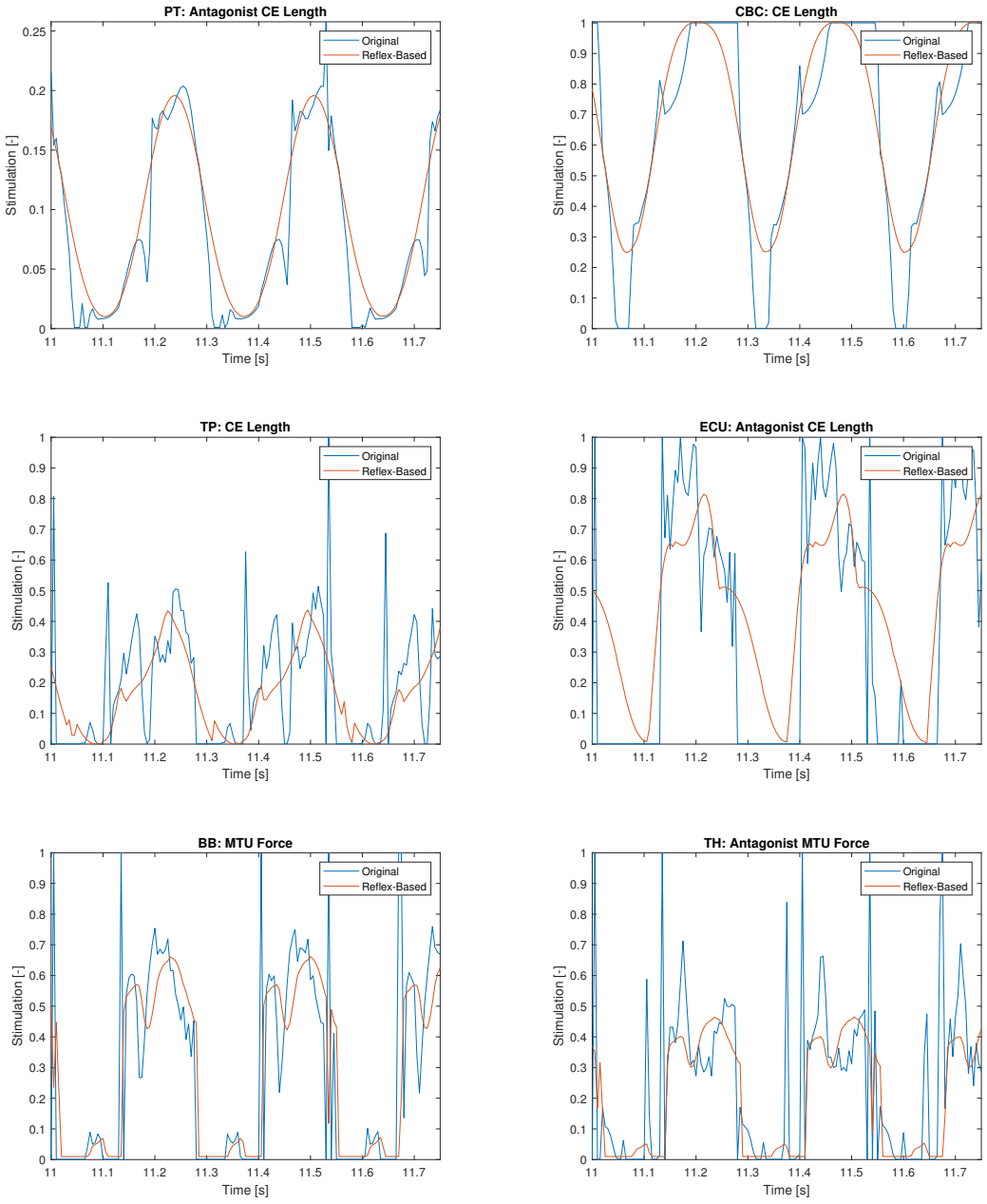

Figure 3.3: The reflex-based stimulation for each muscle using the sensory information selected with table 3.1 is compared to the original stimulation, i.e. the one obtained with the Inverse Hill Model. This part of the analysis has been performed over multiple cycles in order to limit the influence of perturbations.

Case Name	Frequency Multiplier	Amplitude Multiplier
Freq +20%	1.2	0.93
Freq -20%	0.8	1.06
Amp -20%	1.6	0.8
Amp +20%	0.62	1.2

Table 3.3: Multipliers changing the frequency and amplitudes for the flight parameter sensitivity analysis.

Case	$G[m^{-1}]$	$S_0[-]$	$P_{off}[m]$
Amp +20%	-4.77	0.183	0.0769
Freq -20%	-4.82	0.175	0.0799
Standard	-5.72	0.196	0.0811
Freq +20%	-6.82	0.207	0.0826
Amp -20%	-6.90	0.202	0.0853

Table 3.4: *Pectoralis* (PT): The parameters of the reflex-based stimulations are given for increasing wingbeat frequencies.

3.3 Flight Parameter Sensitivity

The sensitivity to flight speed changes is studied in this section. The reader is reminded that the frequency and amplitudes of the movements have both been changed by 20% up and down. Of course, a decrease in frequency will require an increase in amplitude in order to obtain a stable flight altitude. Changes of 20% on the amplitude are bigger than of that same percentage on the frequency. The constant values by which the frequency and amplitudes have been multiplied are shown in table 3.3. The effects of these changes on the different results are analyzed in this section.

First, the muscle forces are compared in the different scenarios in figure 3.4. Next, figure 3.5 shows the effect on the delay and correlation of the Reflex-based Control. The parameters for the reflex-based calculations are in tables 3.4 to 3.9. Figure 3.6 shows the reflex-based stimulations of each flight case, along with their original stimulation from the Inverse Hill Method.

Case	$G[m^{-1}]$	$S_0[-]$	$P_{off}[m]$
Amp +20%	49.16	0.225	0.0528
Freq -20%	56.78	0.215	0.0545
Standard	57.41	0.250	0.0552
Freq +20%	58.23	0.290	0.0560
Amp -20%	58.44	0.360	0.0575

Table 3.5: *Coracobrachialis Caudalis* (CBC): The parameters of the reflex-based stimulations are given for increasing wingbeat frequencies.

Case	$G[m^{-1}]$	$S_0[-]$	$P_{off}[m]$
Amp +20%	47.00	0.01	0.1945
Freq -20%	46.72	0.01	0.1954
Standard	52.43	0.01	0.1959
Freq +20%	53.66	0.01	0.1955
Amp -20%	46.25	0.01	0.1948

Table 3.6: *Tensor Propatagialis* (TP): The parameters of the reflex-based stimulations are given for increasing wingbeat frequencies.

Case	$G[m^{-1}]$	$S_0[-]$	$P_{off}[m]$
Amp +20%	-71.97	0.99	0.1032
Freq -20%	-78.20	0.99	0.1037
Standard	-78.56	0.99	0.1035
Freq +20%	-78.08	0.99	0.1031
Amp -20%	-69.36	0.99	0.1011

Table 3.7: *Extensor Carpi Ulnaris* (ECU): The parameters of the reflex-based stimulations are given for increasing wingbeat frequencies.

Case	$G[m^{-1}]$	$S_0[-]$	$P_{off}[m]$
Amp +20%	0.0129	0.01	0
Freq -20%	0.0124	0.01	0
Standard	0.0135	0.01	0
Freq +20%	0.0131	0.01	0
Amp -20%	0.0117	0.01	0

Table 3.8: *Biceps Brachii* (BB): The parameters of the reflex-based stimulations are given for increasing wingbeat frequencies.

Case	$G[m^{-1}]$	$S_0[-]$	$P_{off}[m]$
Amp +20%	0.0094	0.039	0
Freq -20%	0.0094	0.021	0
Standard	0.0094	0.01	0
Freq +20%	0.0087	0.01	0
Amp -20%	0.0073	0.027	0

Table 3.9: *Triceps Brachii Humeral Head* (TH): The parameters of the reflex-based stimulations are given for increasing wingbeat frequencies.

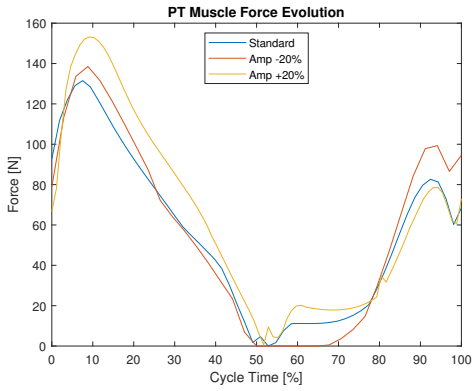

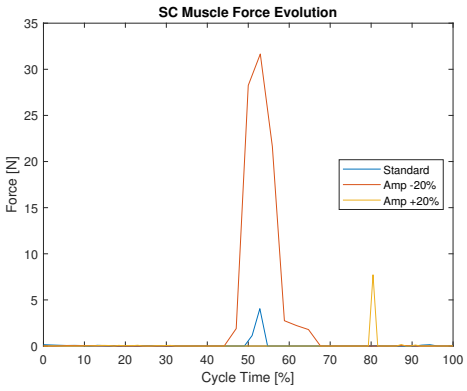

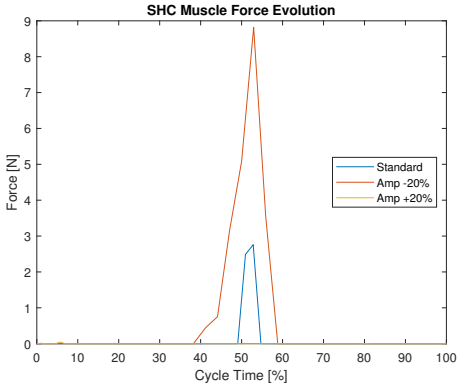

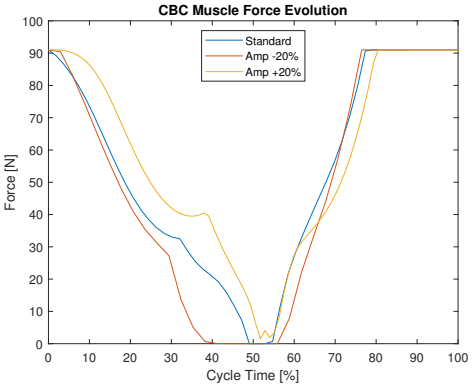

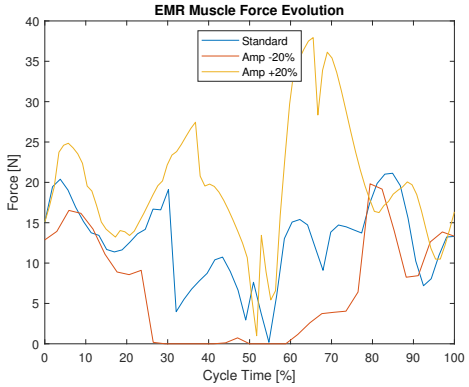
EMR Muscle Force Evolution
Standard
Amp -20%
Amp +20%
Force [N]
Cycle Time [%]

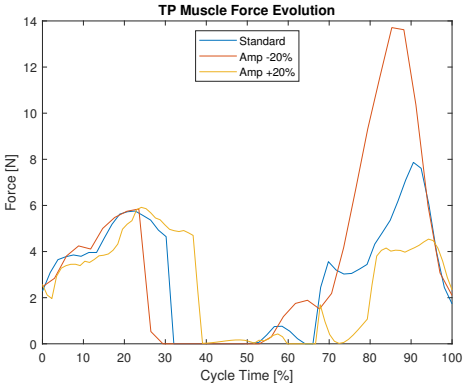
TP Muscle Force Evolution
Standard
Amp -20%
Amp +20%
Force [N]
Cycle Time [%]

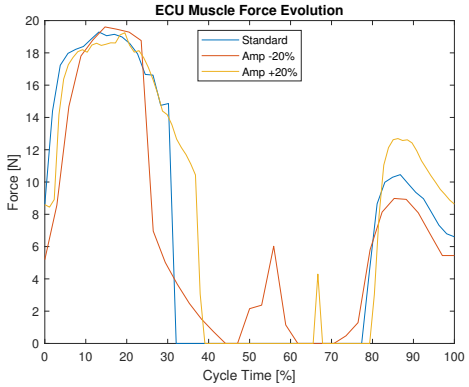
ECU Muscle Force Evolution
Standard
Amp -20%
Amp +20%
Force [N]
Cycle Time [%]

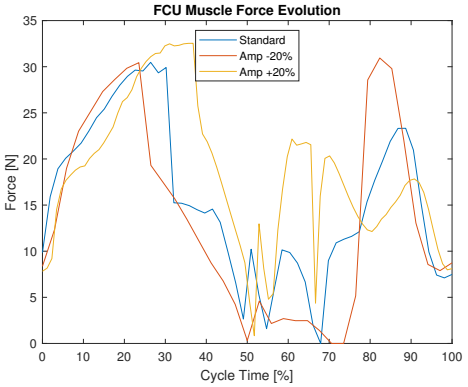
FCU Muscle Force Evolution
Standard
Amp -20%
Amp +20%
Force [N]
Cycle Time [%]

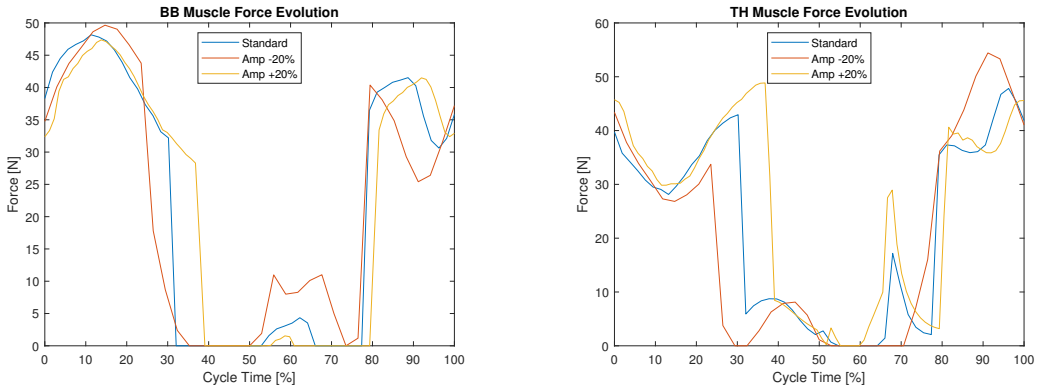

Figure 3.4: Force of the different muscles during one full cycle. A cycle is defined as starting and ending when the wing is fully raised (*Pectoralis* (PT) at maximum length). The standard case is compared to an increase and a decrease of 20% in the movement amplitudes. The changes based on frequency are not shown in order to keep the clarity. The amplitude has been chosen rather than frequency since this gives the largest difference with the standard case.

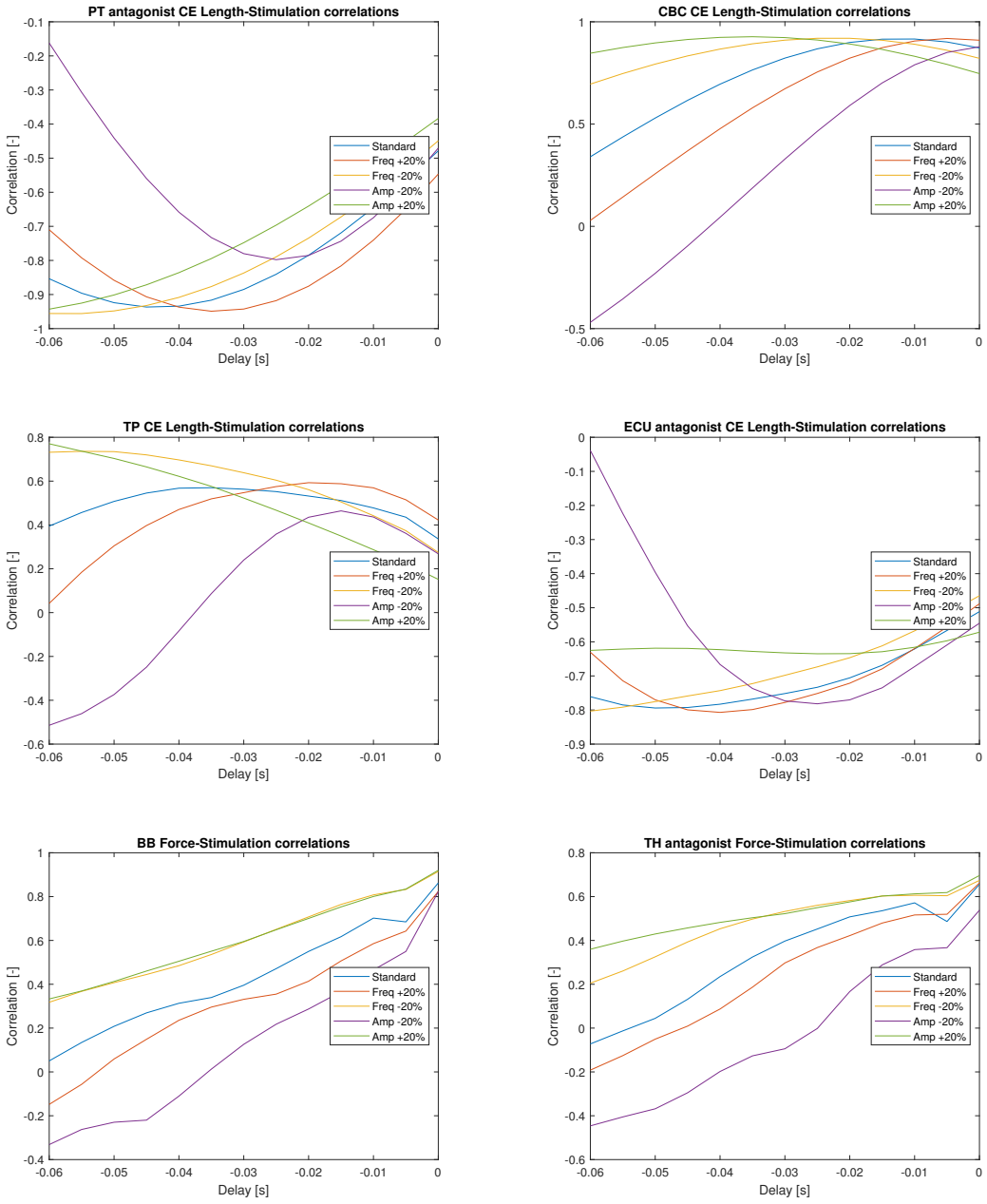

Figure 3.5: The correlations in function of the delay are shown for the different cases for each muscle and sensory information that has been selected previously.

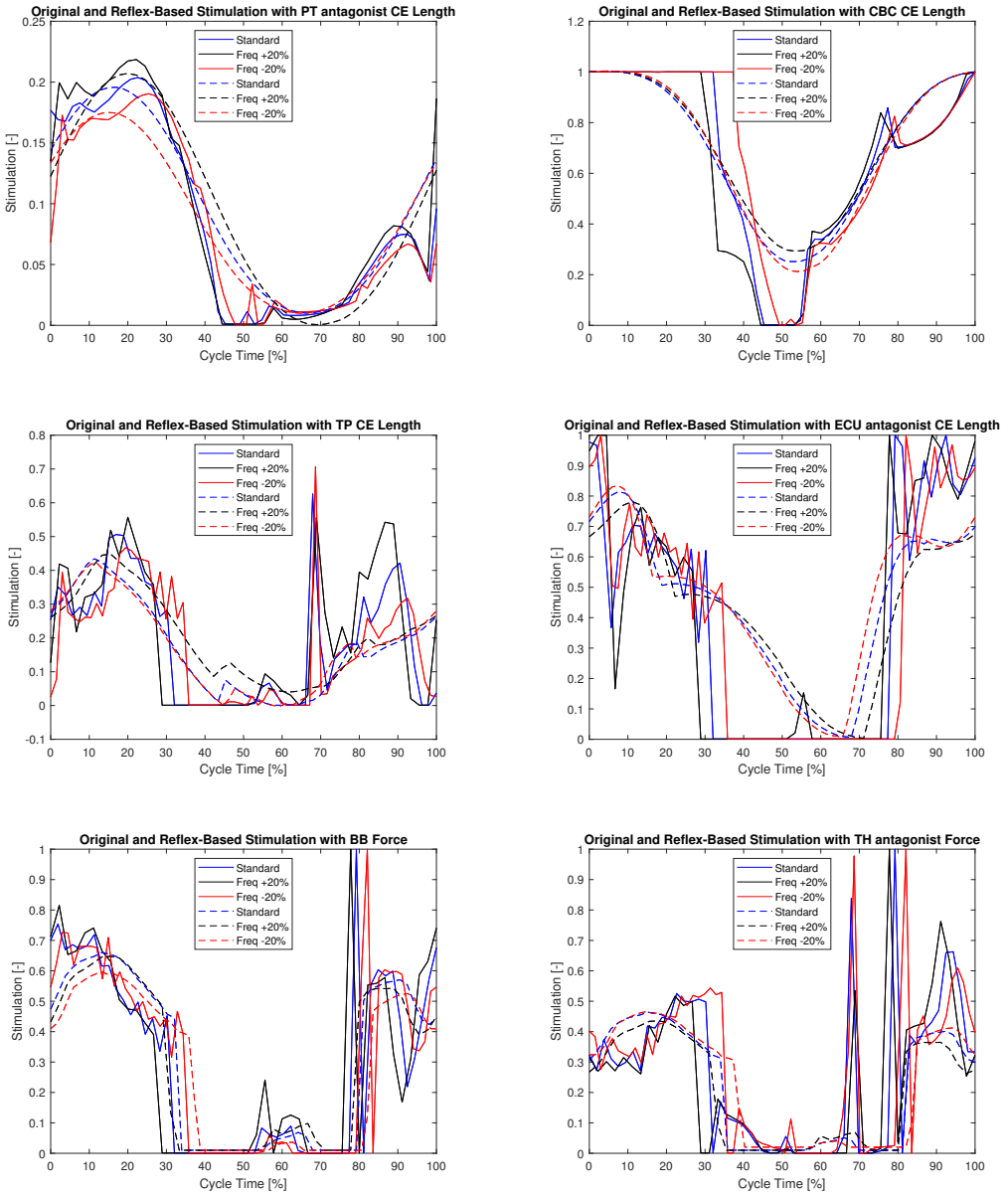

Figure 3.6: Filled lines represent the original stimulations (found with the Inverse Hill Method). The dashed lines show the reflex-based stimulation. One full cycle is represented. Only three cases (standard, frequency increased by 20% and frequency decreased by 20%) are shown in order to maintain clarity. The frequency has been chosen over the amplitude (larger frequency variation) since, as shown in figure 3.5, the optimal delays vary more for more distant frequency values. Since wingbeat frequency remains relatively constant for birds (varies less than 20%) [16], this will be enough to be able to make observations.

Chapter 4

Discussion

4.1 Result Analysis

4.1.1 Muscle-Tendon Unit Force

The MTU force is shown in figure 3.1. While the force shown is technically the muscle force, i.e. the force generated by the contractile element, it is equal to the MTU force since, in this case, F_{pe} and F_{be} are zero by design (as explained in section 2.2.2).

The first observation that can be made, is that the forces found for the muscles *Supracoracoideus* (SC) and *Scapulohumeralis Caudalis* (SHC) are zero most of the time, with some relatively small peaks once per cycle. Their roles, as explained in section 2.1.1, are to raise the wing and abduct the shoulder for the SC, and to raise the wing and adduct the shoulder for the SHC. While they work against each other for a abduction and adduction (which is actually not a movement in this kinematics analysis, see section 2.1.1), they are both used to raise the wing.

During steady-state flight, the lift on the wing will automatically push it upwards, reducing the need for a muscle force. The SC is mostly used for take-off, while being of lesser importance during regular flight [17]. It is still surprising to see an (almost) zero force for these two muscles. Thus can be understood when looking at figure 4.1, showing the torque on the shoulder for the main flapping movement. It is almost always positive, meaning that there is a force needed to pull the wing downwards. When the torque is negative, a force is needed to raise the wing. This is what SC and SHC do. However, this figure shows that the torque is almost never negative, meaning that SC and SHC are not used most of the time. This might indicate that the aerodynamic model overestimates the lift, since there is excess lift to raise the wing. It unfortunately means that not much data will be extracted for these muscles. A more complete aerodynamic model could solve this.

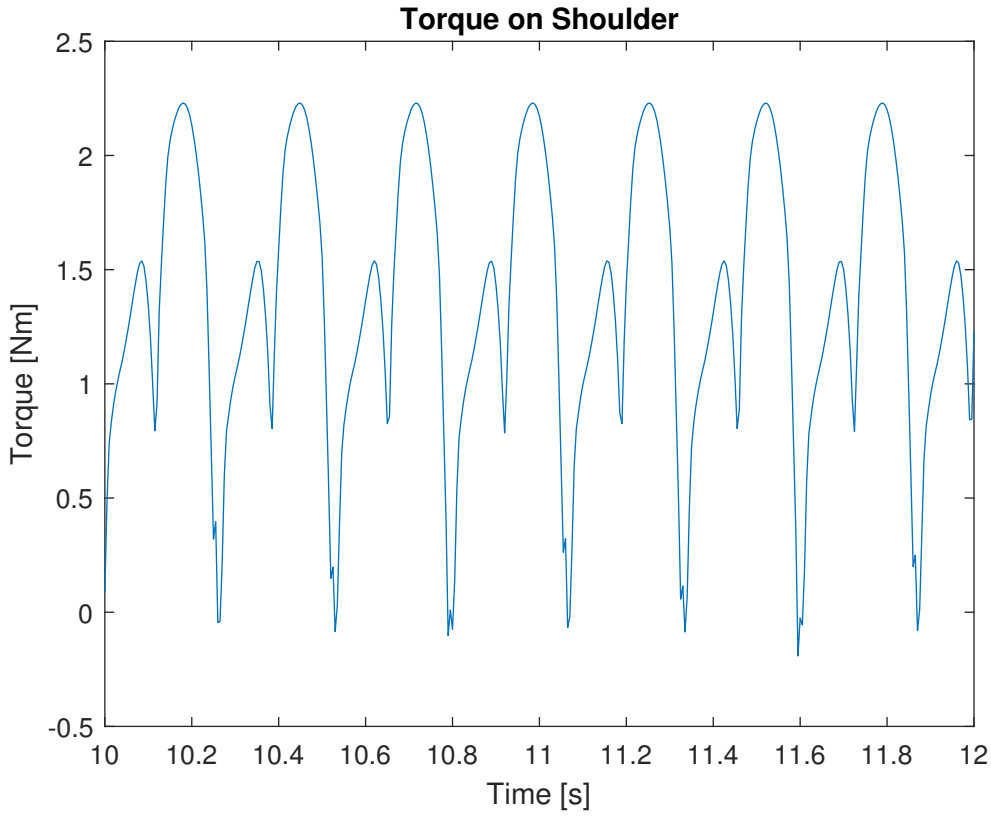

Figure 4.1: Torque on the shoulder for the flapping movement.

While the data have been extracted after 10 seconds of simulation in order to be in a steady state flight (therefore with constant altitude), there are still some differences (spikes) very locally between cycles. These spikes are already present in the torques on the joints given by the Robotran model. However, since they are very narrow (single data points), they do not impact the solutions significantly.

4.1.2 Muscle Force, Activation and Stimulation

Figure 3.1 shows the muscle force, activation, and stimulation of each muscle. In continuation with the observations made in section 4.1.1, the SC and SHC have very small values for these forces, activations and stimulations. More interestingly, the *Coracobrachialis Caudalis* (CBC) has plateaus in its plots. This is due to the muscle reaching its upper bounds as described in section 2.2.3. In that section it is explained that the upper bound for this force is the minimum value between the maximum muscle force, F_{max}, and the product $F_{max} f_v(v_{ce})$.

In the plot showing the muscle force (on figure 3.1), the plateau means that the upper bound condition reached is F_{max}. When the muscle activation reaches a plateau, it means that the upper limit $F_{max} f_v(v_{ce})$ is reached. Since the goal of this separate value for the upper bound is to avoid the activation rising above 1, this works very well. If the upper bound were only F_{max} at all times, then the plateau of the muscle force would be larger, while the plateau of the activation would instead be a peak.

The only other muscle where the second condition is used is the *Extensor Carpi Ulnaris* (ECU). However, this muscle does not reach a plateau. When the force distribution over the different muscles is done without upper bound limiting the activation, the activation becomes higher then 1 (which is not biologically possible). However, when lowering the upper bound in the same way as for CBC, it does not make a plateau, where the force tries to be as high as possible. Instead, it settles at a lower value.

Finally, the stimulations stay almost always between 0 and 1, but as mentioned previously, some spikes leave these limits. This is due to the way the stimulation is found, i.e. by deriving the activation. Since the activation graph is not smooth, it results in high derivatives locally, and thus high (or low) values for the stimulation at those times.

4.1.3 Reflex-based Control

Correlation and Delay

The plots in figure 3.2 show the correlation values between the original stimulation found with the Inverse Hill Method in section 2.2.1 and the different sensory information types used for analysis: muscle force, CE length, and CE velocity (CE is the Contractile Element of the muscle, generating the force, see section 2.2.1). These are taken from both the muscle in question and its antagonist. The purpose of this figure is to easily compare the usefulness of each data type as a source of sensory information. The higher the correlation, the better the match between the data type and the stimulation found by the Inverse Hill Method, which is what needs to be approximated.

The same plots also show us that some muscles do not have any type of data that is close enough (correlation lower than 0.5 in absolute value). Of course, since SC and SHC are not used as much as expected and only generate little force for a small period of time, the stimulation found with the Inverse Hill Method is not good enough, and as such it is not possible to know which data type would be the best match.

This is not the case for the *Extensor Metacarpi Radialis* (EMR) and the *Flexor Carpi Ulnaris* (FCU), but they still do not have any satisfactory data types. While it is possible that these muscles are not controlled by reflex loops, this cannot be concluded yet. There are other data types that could be used, but have not been considered in this study (e.g. the joint position of the articulations of the wing). One may also notice that the frequency of the force is much higher than for other muscles, especially for EMR. This might also be the source of the issue.

For the muscles that do have high enough correlations, there are generally multiple data types that have a correlation which is high enough. In those cases, the highest correlation is taken for further analysis, since this makes it more likely to be used for Reflex-based Control. However, one could consider using multiple types of sensory information at the same time in order to increase the correlation with the original stimulation. This has not been done in this project.

The selected data types and the feedback loops are visualized in figure 4.2. From this figure, it is possible to see that the two elbow muscles BB (biceps) and TH (triceps) use the same source of sensory information: the force of BB.

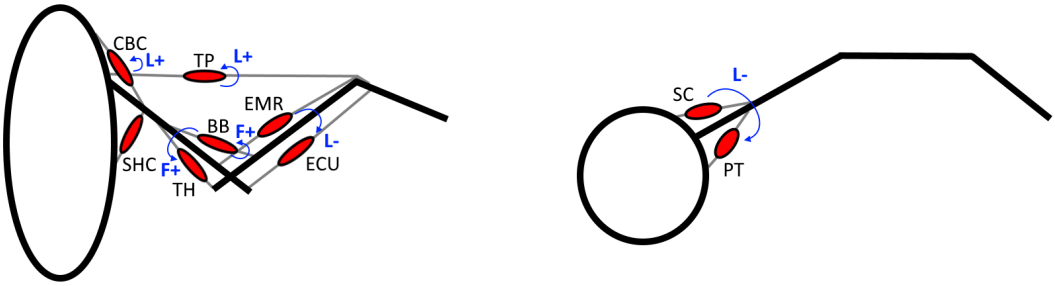

(a) Top view (b) Front view

Figure 4.2: Schematic representation of the feedback loops as indicated by table 3.1. The blue arrows indicate where the sensory information is coming from (same muscle or its antagonist). The blue letters indicate what sensory information is used (F: Muscle force. L: CE length.). The + and - signs indicate whether the gain is positive or negative.

Stimulation Bias and Gain

When looking at the stimulation gain shown in table 3.2, one can observe that for muscles using the own muscle's data (CBC, TP and BB) the gain is positive. For the muscles using antagonist's data (except TH, i.e. PT and ECU) the gain is negative. This makes sense since a negative gain for the length of the antagonist is similar to positive gain for the own muscle's length (their elongations are opposite).

A positive gain for the muscle's own length means that the longer the muscle, the higher the resulting stimulation. This is good for periodic motions: as the muscle gets longer, it needs to contract again. Therefore a higher stimulation is needed. This makes the muscle contract itself, reducing its length. The shorter the muscle gets, the smaller the stimulation becomes, meaning that the muscle contracts with less force. This makes it easier for the antagonist to start contracting, assuming it is controlled by a similar method. This facilitates cyclic movements.

Similarly, the force controlled muscle BB has a positive gain. This means that a higher force results in a higher stimulation. When pulling on a muscle (trying to elongate it), its force is increased, and when pushing on it, the force is decreased. This means that, with a positive gain, pulling on the muscle results in a higher stimulation, which contracts the muscle.

Conversely, trying to shorten the muscle, its force is reduced, leading to lower stimulation (and thus a lower force generated by the muscle). This is very similar to using the muscle length.

With these reflections, one would expect to have a negative gain for TH (which uses its antagonist's muscle force). However, table 3.2 shows that it is positive. This is probably caused by the articulation on which the muscle works, i.e. the elbow, which does not move during flight in this model (see section 2.1.1). This leads to very similar forces for BB and TH, because when one muscle needs to contract, the other needs to do so as well in almost the exact same way in order to insure that the elbow does not rotate.

The similarity between the forces of the muscles, but also their lengths, is shown in figure 3.2. On the plot showing the correlations for TH, the force and length of TH give very similar correlation to the force and length of its antagonist, BB. With the antagonist's force having a slightly higher correlation, this explains why the gain is positive.

This same table shows the stimulation bias S_0 for each case. As explained before (section 2.3.3), these biases are given the value of 0.01 for positive gains and 0.99 for negative ones. This can be seen for the muscles TP, ECU, BB, and TH. The muscles PT and CBC however have different values. The reason for this is also explained in that section.

As a reminder, if the values 0.01 and 0.99 were kept for these muscles, it would result in negative signals $P(t) = l_{ce}(t) - l_{off}$. This is biologically not possible. For this reason, the value of S_0 was increased just enough to have $P_{off} = min(l_{ce}(t))$. This meant that the condition $P(t) \geqslant 0$ was satisfied. S_0 was not increased further, since observation for other muscles (especially BB and TH, which use forces and thus do not have offset values) indicated that lower S_0 are sought.

The plots of figure 3.3 allow a comparison between the target, original stimulation found with the Inverse Hill Method (section 2.2.4) and the reflex-based results. The resemblance is better for some muscles than others, which is expected since they do not all have the same correlation.

When looking at the plots for BB and TH, it is clear that both muscles use the same sensory information P (the muscle force of BB). They do not, however, have the same values for the gain G and the stimulation bias S_0.

Figure 3.3 also shows why S_0 tries to be as close as possible to 0 (or 1) for most

muscles: This allows them to reach closer to 0. Since the original stimulations for most muscles spend a relatively long time at 0, and the reflex-based stimulations try to match it, this is a necessity. As explained before, since $S_0 = 0$ is not biologically possible, the lower limit of 0.01 has been chosen.

4.1.4 Flight Parameter Sensitivity

In order to verify the robustness of the method, flight parameters are modified and the results compared to the original case. In particular, the wingbeat frequency is modified. In order to remain in stable flight conditions (constant altitude), the amplitude of the movements needs to be changed as well.

At first, the frequency was increased and decreased by 20%. This arbitrary value was taken in order not to have too large changes while still being significant enough to make interesting observations.

However, since the corresponding amplitude changes where on the smaller side, new flight parameters were chosen by changing the amplitude by 20% and modifying the frequency as needed.

The resulting sets of frequency and amplitude are shown in table 3.3. It is important to keep in mind, however, that in reality the wingbeat frequency does not vary this much. 20% is already a lot, even for differences between steady-state flight and take-off.

Effect on Forces

The first effect studied is the change in the muscle forces. This is shown in figure 3.4. In order to keep the clarity of the graph, only three cases are shown instead of 5: the standard case, used previously, and the most extreme cases.

A first observation that can be made is for the forces of SC and SHC. These muscles, which raise the wing, were barely used previously (in the standard case). With the higher frequency (case Amp -20%) the muscles are used more. This further indicates that the lift obtained by the simple aerodynamic model used it too high. At higher frequencies, the lift force is not sufficient anymore to lift the wing quickly enough, which is why SC and SHC are being used. Since the figures show the force over one cycle, starting and ending when the wing is fully raised, it can be observed that the SC and SHC are activated when the wing is at its lowest

point, and needs to be raised. This is when the upwards acceleration is the highest.

A second observation that can be made from the same figure is that, as opposed to what one might expect, the force for the standard case is not always in between the higher and lower frequencies. While the general look of all plots are similar, different frequencies use some muscles more than others, and for some muscles the force is higher during one part of the cycle then for another. For example, For the EMR, the *Amp +20%* case has much higher force values than the other ones, while for the TP the force is higher for the *Amp -20%*.

When looking at the PT muscle force, in the first part of the cycle *Amp +20%* has the highest force, but at the end of the cycle it is higher for *Amp -20%*. This high value at the end of the cycle may be for the same reason as why the SC and SHC muscles are high in the middle of the cycle. The end of the cycle is when the wing transitions from going up to going down. This is the part with the largest acceleration and thus requires the highest force.

Effect on Delay

In this section, the effect of the different flight cases on the optimal delay for the reflex-based stimulations are observed. As a reminder, the best outcome would be to have no change in optimal delay between the cases, since the delay is a physiological property and can not be changed by the bird when flying in different conditions.

For the larger frequency changes (cases *Amp +20%* and *Amp -20%*) the delays deviate significantly from the standard case. For the smaller frequency changes however, (cases *Freq +20%* and *Freq -20%*) the optimal delay is relatively close to the standard case. But still not perfect. This is not a big problem since the difference is not too large at frequency changes of 20 %, while in reality the frequency does not vary nearly as much [16].

Additionally, for most muscles the graphs are relatively flat, meaning that for changes in the delay, the correlation does not change very much. This means that if the delay of the standard case is used in cases *Freq +20%* and *Freq -20%*, the correlation will still be almost as good. This is especially true for cases where the frequency does not vary as much as 20 %.

A last, general observation that can be made from these plots is that the higher the frequency, the shorter the optimal delay. This makes sense of course, since when the movements are faster, the reactions need to be quicker and the signals

sent earlier.

Finally, it is important to keep in mind that the kinematic model is very basic. The modifications made to the frequency and amplitudes are even more so. The amplitudes of all movements have been modified by the same multiplier. It is possible that, for example, the shoulder amplitude should be still a bit higher while the wrist flexing/extending amplitude should not increase as much. This has not been examined as the only criterion used is stable flight (constant altitude), but it could have an impact on this analysis at multiple frequencies and amplitudes.

Effect on Stimulation Bias and Gain

The evolution of the stimulation Gain G, bias S_0, and offset value P_{off} for the increasing frequencies is shown in tables 3.4 to 3.9. For PT and CBC (tables 3.4 and 3.5 respectively) the gain increases (in absolute value) as the frequency increases. These two muscles are the main ones, as they lower the wing at the shoulder and thus provide the lift and thrust for the most part.

This relation between the gain and the frequency can be explained by the fact that, as the frequency rises, the amplitude is reduced. Since the reflex-based stimulation for those muscles uses the length of the muscle or of its antagonist, if the amplitude of the movement is reduced, then the gain must be larger in order to obtain a high enough amplitude for the stimulation. This trend however is not extended to the other muscles, and since it is based only on 5 data points per muscle, it should be considered carefully.

The possible reasons why the other muscles do not exhibit this behaviour are multiple. As said previously, the delay used is not optimal for the non-standard cases. This will impact the gain of the stimulation, since the data to match is not what it should be if the optimal data were used. Also, since the amplitude of the movements is different, it affects force-length ($f_l(l_{ce})$) and force-velocity ($f_v(v_{ce})$) relationships (see section 2.2.1).

Additionally, by definition of the optimal length of the muscles (based on the maximum MTU length during the simulation), the optimal length is different for each case. As the frequency increases, the amplitude decreases and thus the optimal length decreases as well. These changes in the different parameters in turn affect the muscle activation, which then affects the stimulation.

A similar observation can be made for the offset value P_{off}. For the muscles PT and CBC, the higher the frequency, the higher P_{off}. However, this is due to the

way P_{off} is found for those muscles. As explained in section 2.3.3, they initially had the value obtained when setting $S_0 = 0.01$ or $S_0 = 0.99$ (depending on the sign of the gain).

However, this resulted in $P(t) = l_{ce} - l_{off} < 0$, which is not biologically possible. To counter this, S_0 was modified in order to not have this problem anymore, i.e. until P_{off} was equal to the minimum value of L_{ce}. Since this minimum value is increased when the amplitude decreases, P_{off} increases when the frequency is increased.

Effect on Stimulation

Finally, the effect on the total stimulation is visible in figure 3.6. On these graphs is shown that, even though the delay is not optimal, the fit between the original stimulation found with the Inverse Hill Model, and the reflex-based one, is relatively good for each case.

This would be even better with smaller frequency changes, as is the case in reality. Only changes of 20% in frequency are plotted, since more cases would reduce the clarity of the plot. These cases were chosen rather than the ones with higher frequency changes since for those the optimal delay was too distant from the standard one and they are further from reality.

Even though the cycles are normalized, there is a noticeable difference between the different frequencies. They do not all have a similar relative distribution of the forces over the cycle, as one could expect. This shows that the frequency has a real impact on the result.

4.2 General Discussion

In addition to the analysis already made for each result separately in section 4.1, some general observations can be made as well. These will be given in this section.

For most muscles, finding the stimulation of the muscles with the Inverse Hill Model went without problems. The only exceptions for this were SC and SHC, which did not have good forces to begin with, probably due to the simplistic aerodynamic model used. However, their stimulations were good considering the forces used as input.

Another difficulty encountered was managing forces too large to obtain an

activation between 0 and 1. This was the case for CBC and ECU. When finding the muscle forces, one needs to keep in mind that the activation also depends on the length and velocity of the muscle, not only on its force.

This is also important to take into account for the lower bound of the muscle force. Even though in regular use of the muscle (when it stays within its length limits) the minimum force is zero, it could also be higher when outside of this regular use zone. This is caused by the extra elements of the Hill Model, F_{pe} and F_{be} which provide passive forces when activated. Thus the minimum force the muscle can have is the one generated by these force elements.

While this was not an issue in this thesis since steady-state flight is considered (where the muscles do not go outside of their designed length range), this has been considered in the code, keeping it relevant for scenarios where the muscles could leave their designed range.

Figure 4.3 illustrates what would happen in such a case. The obtained muscle force is now larger than the one obtained previously (see figure 3.1). In this case, the muscle activation becomes (almost) zero, since the peaks obtained earlier where SC provided force, are now included in the force generated passively by the PE of the muscle. For this reason, it is no longer necessary to activate the muscle. Without surprise, a zero activation gives a zero stimulation.

This project has also shown that it is (for most muscles) possible to use sensory information as the source of the stimulations sent to the muscles in order to generate lift. For the muscles for which this has not been shown (SC, SHC, EMR, and FCU), it does not mean that they can not be controlled by reflexes.

For the SC and SHC, there is no link between the sensory information and the stimulation. This is caused by the stimulation which is probably not correct, because the forces on these muscles are too small (probably due to the aerodynamic model being too simplistic).

For the EMR and FCU, while it is also possible that the stimulations are not correct (possibly due to the kinematic model not being complex enough), it is also possible that other sensory information should be used. Arguments therefor are given in the next two paragraphs.

Firstly, it is possible that the antagonists were not chosen correctly. Since this model has a limited amount of muscles, most muscles work on different degrees of

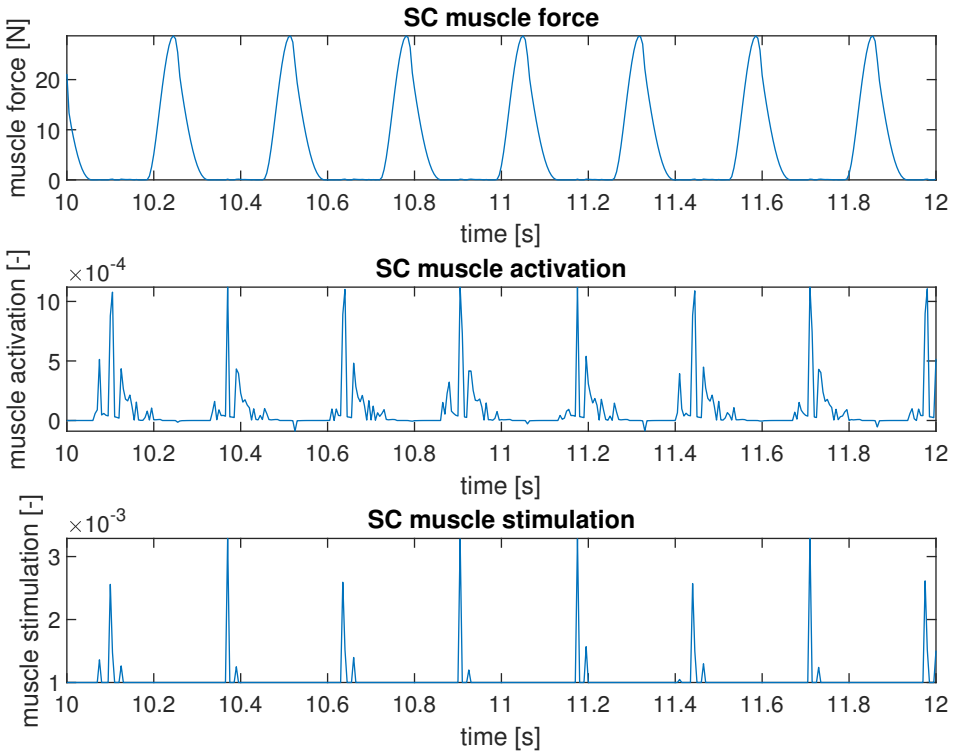

Figure 4.3: Muscle force, activation, and stimulation for the SC muscle when the muscle length exceeds its optimal length. The passive PE (Parallel Element) generates a force, meaning that the muscle force can not be zero, even though the activation is zero. Note that the stimulation has already artificially been limited to not being negative. Without this intervention, there would most likely be a small negative part as well. One should also note that this figure is only used to illustrate what would happen if the optimal muscle length is exceeded. It is not used as a result for the analysis.

freedom in different ways. This means that there are not always clear antagonists for each muscle. However, the muscles where doubt was possible are EMR, FCU, TP, and ECU. For ECU, the optimal sensory information used is given by its antagonist, EMR. For TP, its own CE length was used with a correlation of 0.57. The antagonist's force (FCU) was a close contender with a correlation of 0.53. Although this is very close to the arbitrary limit of 0.5 under which correlations are not considered good enough for analysis. These are arguments in favour of the current choice of antagonists.

Secondly, there are other data types that could be used but have not been studied in this project. An example is the joint position of the different articulations of the wing. This can provide different data sets that could be closer to having a linear relationship with the required stimulation, thus forming a better basis for the Reflex-based Control. Similarly, combinations of sensory information have not been studied either. This could provide a good basis for the Reflex-based Control.

For each muscle in the reflex-based analysis, there is an optimal delay. As mentioned previously, this delay should stay constant in all flight conditions. The delay is observed to be sufficiently constant in this study, since it does not vary much for small frequency changes. There is a large variation for larger changes in frequency, but those do not occur in nature [16]. The goal of this part of the study was thus not to obtain specific results, but to confirm the validity of the previously obtained results, which was successful.

4.3 Limits of the Study

While this study gives a good method for finding the results that were achieved (finding a target muscle stimulation with the Inverse Hill Method, using that target stimulation to identify optimal delay and sensory information for Reflex-based Control, finding the stimulation given by Reflex-based Control, testing robustness of the results), the results themselves need to be taken for what they are.

Since this thesis is part of the first steps in understanding the flight of birds, there are still many steps that need to be explored.This thesis is also based on previous steps that need improvement, since they were themselves even earlier stages than this one.

With better input, like muscle and nervous properties of the targeted bird, an improved aerodynamic model, a more advanced kinematics model, etc. this method and the developed Matlab code can be used with minimal modifications

and provide more precise results.

4.4 Future Perspectives

As mentioned previously, there are multiple things in this project that can be improved. They are listed below and it is explained how they affect the results. Additionally, examples and use cases are presented on how this work can be used in the future for further research.

4.4.1 Improvements

Kinematics Model

The kinematics model, which was made by Guillaume Lamine for his thesis, needs improvements. His work was one of the first building stones of this larger project. He studied the bones and muscles of the wing, built a multi-body model of it, linked it to an aerodynamic model and made a kinematic model of the flight. It was a beginning for the project, but in order to continue these aspects need to be improved and more detailed. It is however very difficult to build a complete kinematic model, especially with the little data available. However, with the results of this thesis, it should be possible to improve it as is explained in section 4.4.2.

One of the possible impacts of the simplistic kinematics model is that the muscle forces, but also the muscle activations and stimulations, are not what they should be. For example, in this model the elbow is considered at a constant angle, but not locked. This means that the constant angle needs to be maintained by the muscles. The main ones for the elbow are BB (biceps) and the TH (triceps). This is the reason why they are activated at the same times with almost opposite forces. This might not be the case if the elbow were moving, giving potentially different results for the forces.

These different results would also impact the stimulation, and potentially change the optimal sensory information. At the moment, the sensory information for TH is the force of its antagonist, BB, with a positive gain. The positive gain for the force of its antagonist is surprising, especially when compared to the other muscles. This might be a consequence of the fixed elbow, and thus of the kinematic model being too simplistic.

With only three movements allowed (wing beating, wrist flexing/extending, and radial/ulnar wrist deviation), it is also possible that the results of other muscles are affected by the simple kinematics model. Either for the same reason as for

TH and BB, or because the length and velocity of the muscles have an impact on the activation computation, and potentially on the force distribution between the muscles.

Aerodynamic Model

The aerodynamic model is a very basic one. It is only a placeholder in this thesis, intended to make the bird fly, but not necessarily accurately. This obviously impacts the results. These indicate that the lift generated by the wings is overestimated, meaning that the aerodynamic force on the wing is enough to lift it for the upstroke, and barely any additional muscle force is required. While the supracoracoideus (SC), which raises the wing, is not supposed to work as much during steady-state flight as during take-off, it is still expected to have some work to do. In these simulations the force needed from that muscle is quite small, showing the need for a better aerodynamic result.

Another indication for this is the relatively low activation of the pectoralis muscle (PT), which is the main source of power during flight. While it can be expected that it does not work at full regime during steady-state flight, its current activation of 20% at maximum seems quite low.

Biological Data

Many approximations have been made for the biological data used. Since the bird of interest, the Bald Ibis, is not very common, there is very little data available about it. For this reason, most data comes from other birds, or even from human walking.

While the precision of some of these parameters (mostly the muscular and nervous properties) does not seem critical for performing the analysis made here (because the method is of importance here, the actual results not as much), it does impact the results. As far as can be said for now, the parameters seem good enough to set up the whole methodology for the goal that is being aimed at by RevealFlight: understand bird flight. If the focus is set on exact results of a specific bird rather then a qualitative understanding of different phenomena at play during flight, there will be a need for better, more precise parameters. These are not available yet, so more research will be needed. These parameters are also the most difficult to determine.

Some other parameters have a bigger impact on the results and the analysis, but would be easier to find. This is probably the case for the musculoskeletal properties.

These include the dimensions of the bones, weights, attachment points of the muscles, optimal lengths, slack lengths of the tendons, etc. These are available for some birds, but not the Bald Ibis, studied here. For this reason, scaling is needed to transform the data. Scaling can be imperfect however, and approximations are needed. Better values for these parameters would give better lever arms for the muscles, meaning that the force distributions between the different muscles would be more accurate.

This may explain why the CBC muscle reaches its maximum value. In this model, it works together with the pectoralis (PT) to lower the wing and provide thrust and lift. With the current layout of the muscles, it is possible that it is taking over work that should be performed by PT, but for which CBC has an advantageous lever arm due to an imprecise model. This could also be caused by the model being too simplistic. If the adduction/abduction degree of freedom of the wing (which is the original role of the CBC) were not locked, it might be used differently and not reach its maximum value for so long.

4.4.2 Future Research

The main goal of this research project was to be usable in further research as part of the RevealFlight project.

The reflex-based study can be used as the basis for a Direct Hill Method. By first using this project to identify sensory information to use in Reflex-based Control, these can be used to create stimulations. These stimulations can be used with the Direct Hill Model to find the muscle force. It will then be possible to verify that the bird flies correctly.

Once that is done, optimization can be used to find better parameters and thus a better flight model. With evolutionary algorithms the wing movements could be more complex, since the program itself tries to find the optimal muscle forces for the right movements. For now, to find the kinematics of the wingbeat, the movements need to be entered manually, which of course limits the complexity of the movements.

Another possibility for further research on the control aspect of bird flight is to implement control by Central Pattern Generators (CPG). These are patterns that generate cyclic outputs for non-cyclic inputs. These can be useful for cyclic motions like bird flight. Since these only have relatively simple inputs and cyclic outputs, they can not manage perturbations. This can be solved by adding Reflex-based Control, which is what has been done here.

Bibliography

[1] J. Hendrickx, P. Chatelain, R. Ronsse. *The RevealFlight project.* https://sites.uclouvain.be/RevealFlight/ 2017

[2] Guillaume Lamine. *Musculoskeletal modelling of the bird.* Master's thesis, Université Catholique de Louvain, 2018

[3] Nicolas Van der Noot. *Rich and Robust Bio-Inspired Locomotion Control for Humanoid Robots.* PhD thesis, École Polytechnique Fédérale de Lausanne Université Catholique de Louvain, 2017.

[4] Harvey I. Fisher, Donald C. Goodman. *The Myology of the Whooping Crane, Grus americana.*

[5] H. Geyer, A. Seyfarth, and R. Blickhan. *Positive force feedback in bouncing gaits?* Proc. R. Soc. Lond. B, vol. 270, pp. 2173–2183, 2003.

[6] Hartmut Geyer and Hugh Herr. *A muscle-reflex model that encodes principles of legged mechanics produces human walking dynamics and muscle activities.* IEEE Transactions on Neural Systems and Rehabilitation Engineering, 18(3), 2010.

[7] A.J. Ijspeert. *Central pattern generators for locomotion control in animals and robots: A review.* Neural Networks 21(4): 642–653. DOI:10.1016/j.neunet.2008.03.014. 2008.

[8] Yan Yang, Huan Wang, and Zihui Zhang. *Muscle architecture of the forelimb of the golden pheasant (chrysolophus pictus) (aves: Phasianidae) and its implications for functional capacity in flight.* Avian Research, 6(1):3, Mar 2015.

[9] Phil Langton. *The [sarcomere] length-tension relation.* 1998. http://www.bristol.ac.uk/phys-pharm-neuro/media/plangton/ugteach/ugindex/m1_index/nm_tension/page2.htm

[10] Marwell Zoo. *Northern bald ibis (Geronticus eremita).* https://www.marwell.org.uk/zoo/explore/animals/65/northern-bald-ibis

[11] Andrew A. Biewener. *Muscle function in avian flight: Achieving power and control.* Philosophical Transactions of The Royal Society B Biological Sciences 366(1570):1496-506, May 2011

[12] Animal Corner. *Golden Pheasant.* https://animalcorner.co.uk/animals/golden-pheasant/

[13] Yasuo Ogawa, Takashi Murayama, Nagomi Kurebayashi. *Ryanodine receptor isoforms of non-Mammalian skeletal muscle.* Department of Pharmacology, Juntendo University, 2002

[14] Wikipedia, *Muscle spindle.* https://en.wikipedia.org/wiki/Muscle_spindle

[15] Daan G.E. Hobbelen, Martijn Wisse. *Limit Cycle Walking, Humanoid Robots, Human-like Machines.* Delft University of Technology, 2007

[16] C. J. Pennycuick, *Wingbeat frequency of birds in steady cruising flight: new data and improved predictions* Journal of Experimental Biology 1996 199: 1613-1618

[17] Kelly M. Kage. *A Portrayal of Biomechanics in Avian Flight.* PhD thesis, Rochester Institute of Technology, 2014

UNIVERSITÉ CATHOLIQUE DE LOUVAIN
École polytechnique de Louvain
Rue Archimède, 1 bte L6.11.01, 1348 Louvain-la-Neuve, Belgique | **www.uclouvain.be/epl**